OXFORD UNIVERSITY PRESS | Molecular Human Reproduction

GSK3A isoform-specific function in human sperm motility

Journal:	*Molecular Human Reproduction*
Manuscript ID	Draft
Manuscript Type:	Original Research
Date Submitted by the Author:	n/a
Complete List of Authors:	Freitas, Maria João; Signal Transduction Laboratory, Institute for Research in Biomedicine – iBiMED, Medical Sciences Department, University of Aveiro Silva, Joana; Signal Transduction Laboratory, Institute for Research in Biomedicine – iBiMED, Medical Sciences Department, University of Aveiro; Reproductive Genetics & Embryo-fetal Development Group; Department of Microscopy, Laboratory of Cell Biology, and Unit for Multidisciplinary Research in Biomedicine (UMIB), Institute of Biomedical Sciences Abel Salazar (ICBAS), University of Porto Brothag, Cameron; Kent State University Department of Biological Sciences Regadas-Correia, Bárbara; CNC.IBILI – Institute for Biomedical Imaging and Life Sciences, Faculty of Medicine, University of Coimbra; CIBIT - Coimbra Institute for Biomedical Imaging and Translational Research, Faculty of Medicine, University of Coimbra; Department Quantitative Methods and Information and Management Systems, Coimbra Business School Fardilha, Margarida; Signal Transduction Laboratory, Institute for Research in Biomedicine – iBiMED, Medical Sciences Department, University of Aveiro Vijayaraghavan, Srinivasan; Kent State University Department of Biological Sciences
Key Words:	sperm motility, sperm biochemistry, Interactome, GSK3

Title: GSK3A isoform-specific function in human sperm motility

Running title: GSK3 function in human sperm motility

M.J. Freitas[1], J. V. Silva[1,2,3], C. Brothag[4], B. Regadas-Correia[5]; M. Fardilha[1*], S. Vijayaraghavan[4].

1. Signal Transduction Laboratory, Institute for Research in Biomedicine – iBiMED, Medical Sciences Department, University of Aveiro, Aveiro, Portugal.

2. Reproductive Genetics & Embryo-fetal Development Group, Institute for Innovation and Health Research (I3S), University of Porto, Porto, Portugal.

3. Department of Microscopy, Laboratory of Cell Biology, and Unit for Multidisciplinary Research in Biomedicine (UMIB), Institute of Biomedical Sciences Abel Salazar (ICBAS), University of Porto, Porto, Portugal

4. Kent State University, Kent, OH 44242, USA.

5. CNC.IBILI – Institute for Biomedical Imaging and Life Sciences, Faculty of Medicine, University of Coimbra, Coimbra, Portugal; CIBIT - Coimbra Institute for Biomedical Imaging and Translational Research, University of Coimbra, Coimbra, Portugal; Department Quantitative Methods and Information and Management Systems, Coimbra Business School, Coimbra, Portugal.

*Correspondence address: Signal Transduction Laboratory, Institute for Research in Biomedicine – iBiMED, Medical Sciences Department, University of Aveiro, Aveiro, Portugal. Tel: +351 234 247 242; E-mail: mfardilha@ua.pt ORCID: 0000-0001-7459-9173

Abstract

Study Question: Does GSK3A present an isoform-specific function in human sperm motility?

Summary answer: GSK3A is a negative modulator of human sperm motility, while GSK3B does not influence sperm motility.

What is known already: In mouse and bovine sperm, GSK3 activity is inversely proportional to motility. Targeted disruption of GSK3A gene in testis results in normal spermatogenesis, but mature sperm present a reduced motility, rendering male mice infertile. On the other hand, GSK3B testis-specific KO is fertile.

Study design, size, duration: Normospermic and asthenozoospermic samples from adult males were used to correlate GSK3 expression and activity levels with human sperm motility profile. Testicular and sperm GSK3 interactome was identified.

Participants/materials, setting, methods: Semen samples from normospermic (n=3) and asthenozoospermic (n=4) donors were collected by masturbation and total GSK3 and serine phosphorylated GSK3 were evaluated using immunoblotting with specific antibodies. GSK3 testis interactome was identified by performing a yeast two-hybrid screen of a human cDNA testis library. GSK3 sperm interactome was characterized by co-immunoprecipitation of GSK3 followed by identification and quantification of its interactors by mass spectrometry. An extensive *in silico* analysis of GSK3 interactome was performed.

Main results and the role of chance: Inhibited GSK3A presents a significant strong positive correlation (r=0.822, p=0.023) with the percentage of progressive human sperm, whereas inhibited GSK3B is not significantly correlated with sperm motility (r=0.577, p=0.175). Regarding subcellular localization of GSK3 isoforms, GSK3A is mainly located in the human sperm flagelum (98%) while GSK3B is primarily localized to the head (97%). The importance of GSK3 in human sperm motility was further reinforced by *in silico* analysis of GSK3 interactome, which revealed a high level of involvement of GSK3 interactors in sperm motility related functions.

Limitations, reasons for caution: The yeast-two hybrid system relies on the yeast cell environment, not fully mimicking mammalian cells. Yet, it is one of the only techniques that indicates binary interactions. Co-Immunoprecipitation does not prove direct interaction, and weak interactions are usually lost but retains intracellular environment conditions

Wider implications of the findings: Our findings prove that human sperm motility relies on isoform-specific functions of GSK3A within this cell. Also, it is in accordance with mouse sperm motility studies. Given the reported relevance of GSK3 protein-protein interactions in sperm motility, we hypothesized that they stand as potential targets for male contraceptive strategies based on sperm motility modulation.

Study funding/competing interest(s): This work was supported by FEDER funds through the "Programa Operacional Competitividade e Internacionalização- COMPETE 2020", by National Funds through the FCT and National Institutes of Health grant. The authors declare that there are no conflicts of interest.

Key words: sperm motility/sperm biochemistry/interactome/GSK3

Introduction

Glycogen synthase kinase 3 (GSK3), a serine/threonine kinase, has been involved in a wide range of cellular processes such as apoptosis, mitosis, and proliferation (Kaidanovich-Beilin and Woodgett, 2011; Beurel *et al.*, 2015). Moreover, deregulation of GSK3 functions has been associated with pathological conditions such as cancer, Alzheimer's disease, and diabetes (Amar *et al.*, 2011; Gao *et al.*, 2011). GSK3 is ubiquitously expressed and is encoded by two genes giving rise to two isoforms: GSK3A and GSK3B. The isoforms differ in their N-termini with GSK3A having a unique glycine-rich N-terminus which is highly conserved in mammals, suggesting an isoform-specific function (Azoulay-Alfaguter *et al.*, 2011).

GSK3 plays a central role in the male reproductive system. In mouse testis, GSK3A is expressed in the seminiferous tubules and its expression increases during the onset of spermatogenesis, peaking in adult testis (Bhattacharjee *et al.*, 2015). GSK3B expression is present in cells entering meiosis, spermatids and Sertoli cells (Guo *et al.*, 2003). Curiously, targeted disruption of GSK3A gene in testis, results in normal spermatogenesis, but mature sperm presented a reduced motility and metabolism, rendering male mice infertile (Bhattacharjee *et al.*, 2015, 2018). On the other hand, GSK3B testis-specific KO was fertile (Bhattacharjee *et al.*, 2018). In mouse and bovine sperm, GSK3 activity is inversely proportional to motility and in immotile caput sperm, GSK3 activity is 6 times higher than that of motile caudal sperm (Vijayaraghavan *et al.*, 1996, 2000). GSK3 activity is controlled by its phosphorylation state. When serine phosphorylated, GSK3 catalytic activity is low (GSK3A Ser9 and GSK3B Ser21) but when tyrosine phosphorylated, it is activated (GSK3A Tyr 279 and GSK3B Tyr 216) (Wang *et al.*, 1994).

Although in bovine and mouse the role of GSK3 in male fertility is well established, in human sperm the knowledge is limited. With that in mind, we performed a GSK3 characterization, by determining its activity levels in asthenozoospermic and normozoospermic ejaculated human samples and subcellular location in human sperm. The observation that mouse GSK3B cannot substitute for GSK3A implies that GSK3A is essential for normal sperm physiology. We considered that the unique role of GSK3A in sperm motility is reliant on its interactors and, as such, identified the GSK3A and GSK3B interactomes in both human testis and sperm.

Methods

Ethical approval

This study was approved by the Ethics and Internal Review Board of the Hospital Infante D. Pedro E.P.E. (Aveiro, Portugal) ((Process number: 36/AO) and was conducted in accordance with the ethical standards of the Helsinki Declaration. All donors signed an informed consent forms allowing the samples to be used for scientific purposes.

All procedures using mice were performed at the Kent State University animal facility and were approved by the National Institute of Environmental Health Sciences institutional Animal Care and Use Committee (IACUC) and the Kent State Animal Ethics Committee under the IACUC protocol number 362DK 13-11. Immediately after CO_2 euthanization, testis and epididymis of 3-4-month-old CD1 mice (*mus musculus*) were removed.

Sperm extracts

Human ejaculate semen samples were obtained from healthy donors by masturbation into a sterile container. Basic semen analysis was performed by qualified technicians according to World Health Organization (WHO) guidelines (Organization, 2010). There was no significant presence of non-sperm cells in the sample (round cells <1.0×10^6 cells/mL). After semen liquefaction, sperm cells were washed in phosphate buffered saline (PBS1x, Fisher Scientific, Loures, Portugal).

Immunoblotting

Washed human sperm were lysed in either Tris buffer (20mM Tris-HCl, pH 7.4, 1mM EDTA, 1mM EGTA) (Fisher Scientific); 1xRIPA (0.05M Tris-HCl, pH 7.4, 0.150M NaCl, 0.25% deoxycholic acid, 1% NP-40, 1mM EDTA) (Millipore Iberica, Madrid, Spain); 1xRIPA modified (0.05M Tris-HCl, pH 7.4, 0.150M NaCl, 0.25% deoxycholic acid, 2% NP-40, 1mM EDTA); or 1%SDS (Fisher Scientific, Loures, Portugal) during 30min on ice and centrifuged at 16,000xG, 15min, 4°C. The supernatant was recovered (protein extract). Mouse sperm cells and testis were lysed in 1xRIPA, centrifuged at

16,000xG, 15min, 4°C and the protein extract recovered. Human testis protein extract was acquired from Takara, Enzifarma, Lisboa, Portugal (ref: 635309).

Sperm protein extracts were mass normalized using BCA assay (ref: 23225, Pierce, Fisher Scientific) separated by SDS-PAGE and electrotransfered to a nitrocellulose membrane. Afterwards, the membrane was incubated with the following antibodies: mouse anti-GSK3A/B (Invitrogen, Fisher Scientific, ref: 44-610, 1:2000) rabbit anti-GSK3A (Cell Signaling Technology, Danvers, MA, USA, ref: #9338, 1:1000) rabbit anti-GSK3B (Cell Signaling ref: #9315, 1:1000); mouse anti-GSK3A pS21 (Santa Cruz Technologies, Heidelberg, Germany, ref: sc-365483, 1:1000); mouse anti-GSK3B pS9 (Santa Cruz Technologies ref: sc-373800, 1:1000) and rabbit anti-LRP6 (Cell Signaling, ref: #2560, 1:1000), 4ºC, ON. Finally, the membrane was incubated with the appropriate infrared secondary antibodies (1:5000, Li-Cor Biosciences UK Ltd, Cambridge, UK). The images were obtained using Odyssey Infrared Imaging Bands System (Li-Cor Biosciences). Bands were quantified with the Quantity One 1-D Analysis Software (Bio-Rad, Amadora, Portugal). Phosphoserine GSK3 levels were calculated by determining the ratio between phosphoserine signal and total GSK3 signal. GSK3 levels were normalized to the loading control Ponceau S. The statistical measures used were the mean and standard error of the mean (SEM). A test of normality (Shapiro- Wilk test) was performed to assess normality of quantitative variables. The Pearson correlation coefficient r was determined to assess the relationship between two variables. Statistical analysis was conducted using the Statistical Package for Social Sciences, version 19 (SPSS ®, Chicago, IL, USA). The significance level was set at 0.05.

Immunocytochemistry

Washed human sperm were spread onto a glass coverslip, allowed to dry and fixed in 4% formaldehyde (Fisher Scientific) for 10 min. After, sperm were permeabilized in 0.1% Tween (Fisher Scientific) in 1% goat serum (Sigma-Aldrich Química, S.A., Sintra) and 5% BSA (NZYTech, Lisboa, Portugal) for 20min. Blocking was performed with 1% goat serum and 5% BSA for 1h30min and then incubated with primary antibodies: rabbit anti-GSK3A (Cell Signaling ref: #9338, 1:50) and rabbit anti-GSK3B (Cell Signaling ref: #9315, 1:50) overnight at 4°C; rabbit anti-LRP6 (Cell Signaling, ref: #2560, 1:50), rabbit anti-pLRP6 1490 (Cell Signaling, ref: #2568, 1:50) and rabbit anti-AKAP11 (Invitrogen, Fisher Scientific, ref: PA5-39868, 1:100) for 1h20min. The sperm cells were incubated with anti-rabbit Alexa 594nm (Life Technologies S.A., Madrid, Spain, 1:800) for 45min at room temperature. Coverslips were washed in PBSx1 + 0.1% Tween, followed by one wash step in PBS1x. Finally, Hoechst was added, and coverslips were mounted onto a glass slide with ProLong™ Gold Antifade Mountant (Invitrogen, Fisher Scientific, ref: 10144). Negative controls were processed in parallel. Fluorescence images were obtained using an Imager.Z1, Axio-Cam HRm camera and AxioVision software (Zeiss, Jena, Germany). Three normospermic human sperm samples were analyzed and around 100 cells per sample were assessed.

Yeast two-hybrid screen

Homo Sapiens GSK3A (NM_019884.2) was subcloned using EcoRI and BamHI (New England Biolabs, Herts, UK) and *Homo Sapiens* GSK3B (NM_002093.3) was subcloned using NdeI and SalI (New England Biolabs) into pAS2-1 plasmid. Both vectors were sequenced to ensure that GSK3A and GSK3B were in frame with Gal-AD. The pAS2-1-GSK3A and pAS2-1-GSK3B vectors were transformed into AH109 yeast strain by a standard lithium acetate method (Clontech, Takara). GSK3A and GSK3B are not cytotoxic to AH109 yeast cells. Expression of GSK3A and GSK3B was confirmed and both proteins did not activate *per se* the reporter genes (Supplementary Figure 1). For library screening, AH109 transformed with either pAS2-1-GSK3A or pAS2-1-GSK3B was mated with yeast strain Y187 expressing human testis cDNA library in pGADT7-Rec (Mate&Plate Library – Human testis ref. 630470, Clontech, Takara) according to manufacture instructions. Half of the mating mixture was plated onto high-stringency medium (Quadruple dropout medium: SD/-Ade/-His/-Leu/-Trp) and the other half onto low-stringency medium (Triple dropout medium: SD/-His/-Leu/-Trp) and the plates were incubated at 30ºC. Colonies obtained in the low stringency plates were replica plated onto medium with X-A-Gal and incubated at 30ºC to check for MEL-1 expression (blue color colonies).

For GSK3A, 93 positive clones were obtained from a total $2.64x10^7$ screened clones. For GSK3B, 54 positive clones were obtained from a total of $2.75x10^7$ screened clones. The Matchmaker Insert Check PCR mix 2 (Clontech, Takara, ref:630497) was used to identify positive clone cDNA. DNA sequence were compared to the GeneBank database to identify the corresponding protein.

Co-immunoprecipitation

$50x10^6$ sperm cells were lysed in 1xRIPA, supplemented with 1mM of Phenylmethylsulfonyl fluoride (PMSF) (Fisher Scientific) and 0.2mM of sodium orthovanadate (Na_3VO_4) (Fisher Scientific) for 60min on ice and centrifuged at 16.000xG, 4°C, 15min. Sperm extracts were pre-cleared using Dynabeads Protein G (ref: 10003D, Invitrogen, Fisher Scientific) and incubated with either rabbit anti-GSK3A (Cell Signaling ref: #9338, 1:50), rabbit anti-GSK3B (Cell Signaling ref: #9315, 1:50) or rabbit anti-IgG (ref: sc-2027, Santa Cruz Technologies) at 4ºC ON with rotation. After incubation, 50µL of dynabeads were added and incubated for 2h. After washing with PBS1x, the dynabeads were resuspended in 50mM glycine (Fisher Scientific) for 5min. Finally, the supernatant was recovered and 1%SDS was added to the dynabeads, incubated 5min, boiled and recovered.

Alternatively, GSK3 antibodies were crosslinked using BS3 (bis(sulfosuccinimidyl)suberate) (Invitrogen, Fisher Scientific, ref: 21580) to Dynabeads Protein G, according to manufacturer instructions. Sperm extracts were pre-cleared and incubated with crosslinked beads for 1h. After washing the beads were resuspended in trypsin digestion buffer (20 mM Tris-HCl pH 8.0, 2 mM $CaCl_2$).

Mass spectrometry

Mass spectrometry studies of GSK3 human sperm interactors were performed in two facilities (two distinct samples).

The Lerner Research Institute's Proteomics and Metabolomics Laboratory: The LC-MS system was a Dionex Ultimate 3000 nano-flow HPLC interfacing with a Finnigan Orbitrap LTQ Elite hybrid ion trap mass spectrometer system. The HPLC system used an Acclaim PepMap 100 precolum (75 µm x 2 cm, C18, 3 µm, 100 A) followed by an Acclaim PepMap RSLC analytical column (75 µm x 15 cm, C18, 2 µm, 100 A). The data was analyzed by using all CID spectra collected in the experiment to search the human UniProtKB protein database with the search programs Sequest and Mascot. Only results with mascot score $p<0.05$ and at least two identifying peptides with mascot ion scores of at least 40 were considered. Specifically, GSK3A and GSK3B sequences searches were performed in Sequest program.

VIB Proteomics Core Facility: The LC-MS/MS system was Ultimate 3000 RSLCnano system in-line connected to a Q Exactive mass spectrometer (Thermo, Fisher Scientific, Loures, Portugal). Peptides were loaded on a reverse-phase column (made in-house, 75 µm I.D. x 20 mm, 3 µm beads C18 Reprosil-Pur, Dr. Maisch). Each sample was injected 3 times and analyzed in triplicate. Data analysis was performed with MaxQuant (version 1.5.6.5) (Cox and Mann, 2008) using the Andromeda search engine with default search settings including a false discovery rate set at 1% on both the peptide and protein level. Spectra were searched against the human proteins in the UniProtKB database (database release version of January 2017). Only proteins with at least one unique or razor peptide were retained. Proteins were quantified by the MaxLFQ algorithm integrated in the MaxQuant software (Cox *et al.*, 2014). A minimum ratio count of two unique or razor peptides was required for quantification. Further data analysis was performed with the Perseus software (version 1.5.5.3) (Tyanova *et al.*, 2016) after loading the protein groups file from MaxQuant. Proteins only identified by site, reverse database hits and contaminants were removed and technical replicate samples of GSK3A, GSK3B, and the negative control were grouped. Proteins with less than three valid values in at least one group were removed and missing values were imputed from a normal distribution around the detection limit. Then, t-tests were performed (FDR=0.0001 and S0=5) to compare samples of GSK3A and GSK3B with the negative control.

In silico analysis

Either UniProtKB or FASTA sequence was retrieved for all GSK3 interactors and used for subsequent *in silico* analysis (only *Homo sapiens* information was considered). The presence of GSK3 consensus phosphorylation site (xxx[ST]xxx[ST]P) (Wu *et al.*, 2009) was analyzed in Eukaryotic Linear Motif (ELM) resource (Dinkel *et al.*, 2016); PhosphoSitePlus (Hornbeck *et al.*, 2015); Kinase Net (http://www.kinasenet.ca); NetPhos 3.1 Server (Blom *et al.*, 2004) ; ScanProsite (de Castro *et al.*, 2006) and GPS 3.0 (Xue *et al.*, 2011). Only data obtained with high threshold, high conservation scores and reported in at least 3 tools were considered. GSK3A and GSK3B interactomes were retrieved from IMEx-curated databases (Orchard *et al.*, 2012) and Human Integrated Protein-Protein Interaction rEference (HIPPIE) database (Alanis-Lobato *et al.*, 2017). Only interactions for human GSK3A and GSK3B with human proteins were considered (March 2018).

Gene expression patterns (mRNA) for all interactors (whether identified in this study or obtained from databases) were retrieved from: The Human Protein Atlas (Uhlén *et al.*, 2015); Pattern Gene Database (PaGenBase) (Pan *et al.*, 2013) Expression atlas EMBL-EBI (68 FANTOM5 project-adult; 32 Uhlen´s Lab and GTEx) (Petryszak *et al.*, 2014); BioGPS (Wu *et al.*, 2016) and UniGene (Pontius *et al.*, 2003). mRNA expression values for all databases (Transcripts per million or fragments per kilobase of exon model per million mapped reads) were retrieved and testis expression values were normalized by calculating the percentage of testis expression taking into account the expression of all tissues. Only interactors that presented more than 50% of expression in testis in at least 2 databases used were considered highly expressed in testis and were classified in three categories: 50-75%, 75-90%, and >90%. Differently expressed proteins in asthenozoospermic samples were collected from peer reviewed papers and compared with GSK3 interactors (Cai *et al.*, n.d.; Chen *et* *al.*, 2009; Li *et al.*, 2010, 2011; An *et al.*, 2011; Jing *et al.*, 2011; Shen *et al.*, 2013b; Amaral *et al.*, 2014; Bhagwat *et al.*, 2014; Salvolini *et al.*, 2014; Zhou *et al.*, 2015; Hashemitabar *et al.*, 2015; Saraswat *et al.*, 2017).

Phenotypes associated with all interactors (genes) were retrieved form Mouse Genome Informatics (MGI) (Eppig *et al.*, 2015) and OMIM (Amberger *et al.*, 2015). Manually curated genes associated with phenotypes of male infertility retrieved from DisGeNet (Piñero *et al.*, 2017), Phenopedia (Yu *et al.*, 2010) and DISEASE database. Altered accessory glands, genetic disorders, sexual behavior and tumor incidence were excluded. Also, GSK3A and GSK3B interactors annotated to testis and sperm physiology on GeneOntology enrichment tool (PANTHER version 12.0, 25 August 2017) (Gene Ontology Consortium, 2015) were classified according to those annotations. GSK3A and GSK3B protein-protein interaction (PPIs) networks were built using Cytoscape v 3.6.0 (Shannon *et al.*, 2003). The inner connections between those proteins were captured. To construct sperm motility and testis related GSK3A and GSK3B PPI networks, GSK3A and GSK3B interactors associated with sperm motility and testis phenotypes were extracted from GSK3A and GSK3B interactome network.

Statistical analysis

The statistical measures used were the mean and standard error of the mean (SEM). A test of normality (Shapiro- Wilk test) was performed to assess normality of quantitative variables. The Pearson correlation coefficient, r, was determined to assess the relationship between two variables. Statistical analysis was conducted using the Statistical Package for Social Sciences, version 19 (SPSS ®, Chicago, IL, USA). The significance level was set at 0.05.

.

Results

GSK3A is required for human progressive spermatozoa motility

Characterization of GSK3 in mouse, bovine and primates sperm is well stablished (Vijayaraghavan *et al.*, 1996, 2000; Smith *et al.*, 1999) . Yet, in human spermatozoa, characterization of GSK3 is deficient. We evaluated the expression and activation of both GSK3 isoforms in human testis and ejaculated human sperm (Figure 1).

Figure 1A shows that GSK3A and GSK3B were expressed in human testis and sperm, similar to what was previously described in mouse and bovine. The levels of inhibited GSK3A and GSK3B (serine phosphorylation) were assessed in human testis and sperm. In human testis, no serine phosphorylated GSK3 was detected, while in human sperm both phosphorylated GSK3 isoforms were detected (Figure 1A.). Moreover, different lysis-buffer strength recovered different amounts of GSK3 in human sperm (Supplementary Figure 2).

To assess the correlation between GSK3 activity with ejaculated sperm motility, total and serine phosphorylated GSK3A and GSK3B (low activity) were evaluated in normospermic and asthenozoospermic samples (see Supplementary Table I for sample information). Total GSK3A and serine phosphorylated GSK3A levels appear to be lower in asthenozoospermic samples compared to normospermic (Figure 1B and C), while expression of total and serine phosphorylated GSK3B appear to be similar in both normospermic and asthenozoospermic samples (Figure 1B and C). Also, Figure 1D shows that there was a significant strong positive correlation ($r=0.822$, $p=0.023$) between the percentage of progressive sperm and the levels of inhibited GSK3A, whereas inhibited GSK3B is not significantly correlated with sperm motility ($r=0.577$, $p=0.175$). Although the levels of total GSK3 were not significantly correlated with the percentage of progressive motility, GSK3A presented an apparent positive correlation with the percentage of progressive motile spermatozoa, while GSK3B a negative correlation (Figure 1E). The correlation between GSK3 levels and the percentage of immotile spermatozoa was also analysed, and the results comply with the previous described (Supplementary table II).

GSK3A and GSK3B have distinct distributions in human spermatozoa

The subcellular localization of GSK3A and GSK3B in ejaculated human sperm was analysed. Figure 2 shows that GSK3A was primarily located in the flagellum (98.0%) and 75.7% of sperm cells also showed immunoreactivity in the head. Curiously, 24.2% of the spermatozoa showed a strong immunoreactivity for GSK3A in the equatorial region, particularly at the edges. In contrast, GSK3B was mainly located in the sperm head (97.0%), 23.9% of sperm showed GSK3B distributed throughout the entire head and flagellum and in 76.0% of sperm cells it was present only in the sperm head (Figure 2). Within the flagellum, both GSK3A and GSK3B present a punctured like staining.

GSK3 human testis and sperm interactome

A yeast two-hybrid screen of a human cDNA testis library revealed 46 putative interactors for GSK3A and 21 for GSK3B (Supplementary Table III and IV, respectively). For GSK3A, 76% were new putative interactors while 24% were previously described as GSK3 interactors. 58.7% of GSK3A interactors identified contained the GSK3 consensus phosphorylation site (xxx[ST]xxx[ST]P). Finally, 34.8% of GSK3A interactors were already described to be present in either testis and/or sperm of mammals. For GSK3B, 77.8% were identified for the first time as GSK3B putative interactors. Around 38% of the GSK3B identified interactors had the GSK3 consensus phosphorylation site and 61.1% were previously reported to be present in testis and/or sperm of mammals.

GSK3A and GSK3B interactors were isolated from ejaculated human sperm by co-immunoprecipitation using isoform-specific GSK3 antibodies in two independent experiments by mass spectrometry analysis. Endogenous GSK3A and GSK3B were successfully immunoprecipitated in both experiments (Supplementary Figure 3) and five GSK3A peptides and four GSK3B peptides were identified in mass spectrometry (Supplementary Table V). Note that neither GSK3A nor GSK3B were detected in the negative control. Seventeen and 34 interactors were identified as sperm GSK3A and GSK3B interactors, respectively (Supplementary table V and VII, respectively). Regarding GSK3A interactors, 82.4% were potentially novel interactors and 17.6% contained the GSK3 consensus phosphorylation site. Also, 58.8% of GSK3A identified interactors were described as expressed in either mammalian testis and/or sperm by previous studies. For GSK3B interactors, 85.3% were new putative interactors and 47.1% were shown to be expressed in either mammalian testis and/or sperm. Finally, the GSK3 consensus phosphorylation site was present in 14.7% of GSK3B interactors.

GSK3 interactomes are associated with sperm motility and testis functions

To enrich the GSK3 human testis and spermatozoa interactome, GSK3A and for GSK3B interactomes were retrieved from public available databases. Seventy-five GSK3A interactors and 413 GSK3B have been previously identified (Supplementary table VIII and IX, respectively). With the goal of identifying key GSK3 interactors for sperm and testis physiology, gene expression for GSK3 interactors was retrieved from 5 different tissue-expression databases (Supplementary Table VIII and IX). Four GSK3A interactors are testis-enriched, with more than 90% of their expression restricted to testis: DDI1, GOLGA6C (testis interactors), ACR and PRSS37 (sperm interactors). Although not testis-enriched, TTC16 expression is enhanced in testis (Supplementary Table X). For GSK3B interactors, besides ACR and PRSS37, TEKT5, CMTM2 (testis interactors), HIST1H1T, PRKACG, TSKS (databases interactors) were classified as highly enriched in testis and CABYR expression is enhanced in testis (Supplementary Table X). To further characterize the GSK3 interactome, differently expressed proteins in asthenozoospermic samples were retrieved from proteomics studies. Overall, eleven GSK3 testis or sperm interactors are increased, eight are decreased and one has conflicting reports in asthenozoospermic samples (Supplementary Tables III, IV, VI and VII).

Protein-protein interaction networks were constructed using data obtained from this study and retrieved from databases. The GSK3A interactome network (Supplementary Figure 4) presents 130 proteins, including GSK3A. Between GSK3A interactors 257 interactions are formed. The GSK3B interactome is composed by 456 proteins that form 1813 interactions among them (Supplementary Figure 5).

To add biological meaning to the GSK3 interactome, phenotype and Gene Ontology information were retrieved (Supplementary Table XI and XII). Here, two subnetworks were extracted: sperm motility- and testis-related GSK3-based networks. Twenty-six GSK3A interactors have been associated with motility-related functions, phenotypes and/or subcellular locations (Figure 3). From those, five (PRSS37; DRC1; RPS19; HSPA5 and AP3D1) were identified in this study as GSK3A interactors and only one was classified as testis-enriched protein (PRSS37). PRKACA and DRC1 stand out by presenting five motility-related annotations followed by GLI3 with four. Note that GSK3A itself has been associated with locomotion and cell motility processes. For GSK3B, 100 interactors are annotated to motility-related categories, and from those six are highly expressed in testis (CABYR, TEKT5, PRKACG, PRSS37, TSKS, CMTM2) (Figure 3).

Analysing the GSK3 testis subnetwork (Figure 4), ten GSK3A interactors were associated with testis-related annotations and two of those were identified in this study (PRSS37 and HSP90AA1) (Figure B2.8). Only PRSS37 was described as highly expressed in testis (Figure B2.8). With five testis-related annotations, we highlight AKAP9 and AR. For testis-related categories, GSK3B presents 45 interactors related to testis-related categories (Figure 4).

Although not directly related to sperm motility and testis function, several GSK3 interactors are associated to more general annotations linked to the male reproductive system (Supplementary Figure 6).

AKAP11 and LRP6 subcellular localization in human sperm

Two GSK3 interactors identified in this study, A-kinase anchor protein 11 (AKAP11) and low-density lipoprotein receptor-related protein 6 (LRP6), were chosen for further characterization, since they have been previously involved in male reproduction. Figure 5A shows that LRP6 is present in human testis and sperm at 180kDa, the expected molecular weight of the protein. The band at the higher molecular weight could be due to post translational modification, such as phosphorylation and N-glycosylation, known to occur in LRP6 (Khan *et al.*, 2007; Niehrs and Shen, 2010). Immunocytochemistry studies (Figure 5B), revealed that total LRP6 is localized to the entire length of the flagellum and occasionally at the post-acrosomal area. However, phosphorylated LRP6 (p1490LRP6) is restricted to the midpiece. Moreover, a closer analysis showed that not all sperm cells present immunoreactivity towards LRP6 and p1490LRP6. Only 18% and 29% of sperm cells present immunoreactivity for LRP6 and p1490LRP6, respectively (Figure 5B). Regarding AKAP11, this protein is localized on the anterior portion of the head and the equatorial area of ejaculated human sperm (Figure 5B).

Discussion

GSK3 has been long associated with sperm motility acquisition and maintenance in mammals (Somanath *et al.*, n.d.; Smith *et al.*, 1999; Vijayaraghavan *et al.*, 2000). Recently, an isoform-specific function of GSK3A in mice sperm primary motility acquisition has been suggested. However, the characterization of both GSK3 isoforms (GSK3A and GSK3B) in human sperm and testis physiology has been sparse. Assessment of a similar isoform-specific function of GSK3A in human sperm motility acquisition is thus necessary. This work aimed to characterize GSK3 isoforms in human sperm as well as identify and analyse GSK3A and GSK3B interactome in human sperm and testis. Ultimately, this can help decipher the role of isoform-specific functions of GSK3 in human sperm physiology.

In this study we proved that mature human sperm cells are unique in their need for GSK3A isoform to achieve progressive motility. Similar to other mammals, both GSK3 isoforms are present in human testis and sperm (Figure 1). Characterization of GSK3 levels in normospermic and asthenozoospermic samples proved that in ejaculated human sperm serine phosphorylated GSK3A presents a strong positive correlation with progressive sperm motility, but serine phosphorylation GSK3B does not show any correlation with sperm motility (Figure 1). Furthermore, correlation between the percentage of immotile spermatozoa (Supplementary Table II) and levels of serine phosphorylated GSK3A is in accordance with the correlation observed with progressive motile spermatozoa. This shows that GSK3A activity is strongly correlated with human sperm motility, being a negative modulator, while GSK3B appears does not influence sperm motility. This is the first observation that GSK3 activity is associated with human sperm motility and that this function is a GSK3A isoform-specific function. The power of the study was limited by the relatively small samples size (3 normozoospermic samples and 4 asthenozoospermic samples) However, recent studies reinforce the results obtained. Using, *knock out* technology a GSK3A isoform-specific function in mice sperm motility has been proved by Bhattacharjee and colleagues (Bhattacharjee *et al.*, 2015, 2018).

A possible explanation for the inability of GSK3B to substitute for GSK3A in human sperm relies in a distinct spatial expression pattern between GSK3 isoforms in human sperm cells. The immunocytochemistry studies performed, showed that GSK3A is primarily located in the tail and GSK3B in the head of human spermatozoa. A more plausible explanation for isoform-specific function of GSK3 in human sperm is GSK3 isoform-specific interactors that bind, target and modulate each isoform in human sperm. Work by Zeidner et al., showed that RACK1 is a GSK3A isoform-specific interactor in the central nervous system, and that this interaction requires the unique glycine rich GSK3A N-termini (Zeidner *et al.*, 2011).

With the purpose of identifying GSK3 isoform-specific interactions in the male reproductive system, the GSK3A and GSK3B interactomes in human testis and sperm were identified and characterized (Supplementary Tables III, IV, VI and VII). Due to technical restrains (human testis availability and sperm physiology), the human testis GSK3 interactome was constructed using an yeast two hybrid approach, while for human sperm GSK3 interactome co-IP followed by mass spectrometry was undertaken. The yeast-two hybrid system relies on the yeast cell environment, not fully mimicking mammalian cells. Yet, it is one of the only techniques that indicates binary interactions. Co-Immunoprecipitation does not prove direct interaction, and weak interactions are usually lost but retains intracellular environment conditions. Approximately 27% of the GSK3 interactions identified in this study have been previously described, which results in high confidence in the GSK3 interactomes identified. Furthermore, the interaction between GSK3 and AXIN2 was acknowledged, for the first time, in testis. This interaction is extensively described in somatic cells (Stamos and Weis, 2013; Voronkov and Krauss, 2013; Song *et al.*, 2014; Pronobis *et al.*, 2015), reinforcing our confidence in the results obtained for the GSK3 interactome.

With the purpose of constructing the most complete GSK3 interactome, GSK3 interactions available on PPIs databases were retrieved and GSK3-centered networks were constructed (Supplementary Figures 4 and 5). To identify GSK3 interactions key for sperm physiology (more specifically sperm motility), tissue-expression, phenotypes and gene ontology annotations were integrated into the GSK3 networks. It may be noted that the knowledge of protein tissue expression is still limited and typically does not take into account tissue-specific alternatively spliced transcripts. This is particularly relevant for testis, since testis is the tissue with a higher number of alternative transcripts splice variants (Elliott and Grellscheid, 2006; Uhlén *et al.*, 2015). None of GSK3A interactors listed on databases showed a testis-specific or -enriched expression. We identified the first testis-enriched or -specific GSK3A interactors which reflects the importance for deepening the knowledge on sperm physiology of our results. Regarding GSK3A interactions, 20.1% have a motility related annotation and for GSK3B 21% of interactors have been previously link to cell motility. This is relevant considering the sperm cells are the only human cells that possesses a progressive motile function. The fact that almost a quarter of GSK3 interactome may be involved in the motility cell function reflects that the molecular mechanisms that control sperm cell motility are still partially unknown. Focusing on GSK3A interactions that may have a prominent role in sperm motility we highlight PRSS37. This protein is the only GSK3A interactor that is known to be associated with sperm motility, testis annotations, and categorized as enriched in testis (Figure 3). Previous studies demonstrated that when PRSS37 is absent in mice testis, fertilization is compromised due to inadequate spermatogenesis, decreased sperm oviduct-migration, and decreased sperm-zona binding (Shen *et al.*, 2013a). Concerning testis functions, our analysis revealed that AR, PPP1CC, and AKAP9 appear to have a prominent role since germ cells and other types of testicular cells are greatly affected by their absence (Figure 4). These findings are in accordance with former studies (Varmuza *et al.*, 1999; Wang *et al.*, 2009; Schimenti *et al.*, 2013).

LRP6 and AKAP11, two GSK3 interactors identified in this study, were chosen for further characterization, as being previously involved in male reproduction. LRP6 was already described as involved in sperm motility and testis physiology, and AKAP11 in mouse spermatogenesis (Reinton *et al.*, 2000; Koch *et al.*, 2015)**.** While the interaction between AKAP11 and GSK3B has been previously described (Tanji *et al.*, 2002), to our knowledge this is the first description of the interaction with GSK3A and the first time the interaction is described in human testis. Opposing to earlier studies in human sperm (Reinton *et al.*, 2000), we showed that AKAP11 is localized in the anterior portion of the head and equatorial region (Figure 5B). In somatic cells, AKAP11 has been associated with cell migration (Logue *et al.*, 2011) and in 2002, Tanji et al showed that AKAP11, PPP1, PRKACA, and GSK3B formed a multimeric complex in which PPP1 and PRKACA controlled GSK3B activity. Since both PPP1 and PRKACA have been extensively described in mammalian testis and sperm (Smith *et al.*, 1996; Davidson *et al.*, 2005; Schimenti *et al.*, 2013), we may assume that similar multimeric complex may be formed to control GSK3 activity.

Bioinformatics analysis revealed that in mice, LRP6 absence correlates to male infertility (Supplementary Figure 6 and Supplementary Table XI). Expression studies showed that LRP6 is present in human testis and sperm and is localized along the entire flagellum (Figure 5A and B). Furthermore, when LRP6 is phosphorylated on S1490 (in somatic cells a GSK3 substrate (Davidson *et al.*, 2005; Zeng *et al.*, 2005)) its subcellular location is restricted to the human sperm midpiece (Figure 5B). This is in accordance to earlier studies in mice and bovine sperm (Koch *et al.*, 2015). Interestingly, only a small percentage of the sperm cells within the same sample present staining for both LRP6 and S140 phosphorylated LRP6. Further studies to understand why this expression pattern occurs may prove useful. In 2015, Koch et al explored the non-genetic effects of B-catenin signaling on human sperm and suggested that the interaction between LRP6 and GSK3 is required for protein stabilization and consequently sperm motility (Koch *et al.*, 2015). Therefore, despite the fact that in somatic cells GSK3/LRP6 interaction is involved in gene expression, our results reinforce that in human sperm this interaction can be fundamental for sperm physiology.

In conclusion, our data revealed an isoform-specific need for GSK3A in human progressive sperm motility modulation. The GSK3 interactome identified in this work uncoveres the extent to which GSK3 can be involved in sperm motility and reveals new potential players in the molecular mechanism of sperm motility. Even more, study of GSK3A interactors such as PRSS37 deserve to be pursuit since the likelihood of this protein being involved in sperm motility is high. Furthermore, Although we attempted to identify specific GSK3A interactors, no interaction was validated as GSK3A-unique. Selective GSK3A inhibitors and identification of specific targets of GSK3A can facilitate the development of a new group of male contraceptives based on sperm motility arrest.

Supplementary data

Supplementary data are available at

Acknowledgments

We would like to thank Dr. Phiel for providing the original vector containing the GSK3A and GSK3B ORF.

Author´s Roles

M.J.F designed the study, performed experiments, acquired, analysed and interpreted the data and produced the manuscript. J.V.S performed experiments, interpreted the data and drafted the manuscript. C.B performed experiments and analysed the data. B.R.C analysed and interpreted the data (statistical analysis). M.F and S.V designed the study, analysed and interpreted the data. All authors critically revised the manuscript and approved the final version.

Funding

This work was financed by FEDER funds through the “Programa Operacional Competitividade e Internacionalização- COMPETE 2020” and by National Funds through the FCT- Fundação para a Ciência e Tecnologia (PTDB/BBB-BQB/3804/2014). We are thankful to Institute for Biomedicine – iBiMED (UID/BIM/04501/2013 and POCI-01-0145-FEDER-007628) for supporting this project. iBiMED is supported by the Portuguese Foundation for Science and Technology (FCT), Compete2020 and FEDER fund. Also, this worked was financed by the NIH grant R15 HD068971-01. Image acquisition was performed in the LiM facility of iBiMED, a node of PPBI (Portuguese Platform of BioImaging): POCI-01-0145-FEDER-022122. This work was also supported by an individual grant from FCT of the Portuguese Ministry of Science and Higher Education to M.J.F. (SFRH/BD/84876/2012).

Conflict of interest: The authors declare that there are no conflicts of interest.

References

Alanis-Lobato G, Andrade-Navarro MA, Schaefer MH. HIPPIE v2.0: enhancing meaningfulness and reliability of protein-protein interaction networks. *Nucleic Acids Res* 2017;**45**:D408–D414.

Amar S, Belmaker RH, Agam G. The possible involvement of glycogen synthase kinase-3 (GSK-3) in diabetes, cancer and central nervous system diseases. *Curr Pharm Des* 2011;**17**:2264–2277.

Amaral A, Paiva C, Attardo Parrinello C, Estanyol JM, Ballescà JL, Ramalho-Santos J, Oliva R. Identification of proteins involved in human sperm motility using high-throughput differential proteomics. *J Proteome Res* 2014;**13**:5670–5684.

Amberger JS, Bocchini CA, Schiettecatte F, Scott AF, Hamosh A. OMIM.org: Online Mendelian Inheritance in Man (OMIM®), an online catalog of human genes and genetic disorders. *Nucleic Acids Res* 2015;**43**:D789-98.

An C-N, Jiang H, Wang Q, Yuan R-P, Liu J-M, Shi W-L, Zhang Z-Y, Pu X-P. Down-regulation of DJ-1 protein in the ejaculated spermatozoa from Chinese asthenozoospermia patients. *Fertil Steril* 2011;**96**:19–23.e2.

Azoulay-Alfaguter I, Yaffe Y, Licht-Murava A, Urbanska M, Jaworski J, Pietrokovski S, Hirschberg K, Eldar-Finkelman H. Distinct molecular regulation of glycogen synthase kinase-3alpha isozyme controlled by its N-terminal region: functional role in calcium/calpain signaling. *J Biol Chem* 2011;**286**:13470–13480.

Beurel E, Grieco SF, Jope RS. Glycogen synthase kinase-3 (GSK3): regulation, actions, and diseases. *Pharmacol Ther* 2015;**148**:114–131.

Bhagwat S, Dalvi V, Chandrasekhar D, Matthew T, Acharya K, Gajbhiye R, Kulkarni V, Sonawane S, Ghosalkar M, Parte P. Acetylated α-tubulin is reduced in individuals with poor sperm motility. *Fertil Steril* 2014;**101**:95–104.e3.

Bhattacharjee R, Goswami S, Dey S, Gangoda M, Brothag C, Eisa A, Woodgett J, Phiel C, Kline D, Vijayaraghavan S. Isoform specific requirement for GSK3α in sperm for male fertility†. *Biol Reprod* 2018;

Bhattacharjee R, Goswami S, Dudiki T, Popkie AP, Phiel CJ, Kline D, Vijayaraghavan S. Targeted disruption of glycogen synthase kinase 3A (GSK3A) in mice affects sperm motility resulting in male infertility. *Biol Reprod* 2015;**92**:65.

Blom N, Sicheritz-Pontén T, Gupta R, Gammeltoft S, Brunak S. Prediction of post-translational glycosylation and phosphorylation of proteins from the amino acid sequence. *Proteomics* 2004;**4**:1633–1649.

Cai Z-M, Gui Y-T, Guo X, Yu J, Guo L-D, Zhang L-B, Wang H, Yu J. Low expression of glycoprotein subunit 130 in ejaculated spermatozoa from asthenozoospermic men. *J Androl***27**:645–652.

Castro E de, Sigrist CJA, Gattiker A, Bulliard V, Langendijk-Genevaux PS, Gasteiger E, Bairoch A, Hulo N. ScanProsite: detection of PROSITE signature matches and ProRule-associated functional and structural residues in proteins. *Nucleic Acids Res* 2006;**34**:W362-5.

Chen J, Wang Y, Xu X, Yu Z, Gui Y, Cai Z. [Differential expression of ODF1 in human ejaculated spermatozoa and its clinical significance]. *Zhonghua Nan Ke Xue* 2009;**15**:891–894.

Cox J, Hein MY, Luber CA, Paron I, Nagaraj N, Mann M. Accurate proteome-wide label-free quantification by delayed normalization and maximal peptide ratio extraction, termed MaxLFQ. *Mol Cell Proteomics* 2014;**13**:2513–2526.

Cox J, Mann M. MaxQuant enables high peptide identification rates, individualized p.p.b.-range mass accuracies and proteome-wide protein quantification. *Nat Biotechnol* 2008;**26**:1367–1372.

Davidson G, Wu W, Shen J, Bilic J, Fenger U, Stannek P, Glinka A, Niehrs C. Casein kinase 1 gamma couples Wnt receptor activation to cytoplasmic signal transduction. *Nature* 2005;**438**:867–872.

Dinkel H, Roey K Van, Michael S, Kumar M, Uyar B, Altenberg B, Milchevskaya V, Schneider M, Kühn H, Behrendt A, *et al.* ELM 2016--data update and new functionality of the eukaryotic linear motif resource. *Nucleic Acids Res* 2016;**44**:D294-300.

Elliott DJ, Grellscheid SN. Alternative RNA splicing regulation in the testis. *Reproduction* 2006;**132**:811–819.

Eppig JT, Richardson JE, Kadin JA, Ringwald M, Blake JA, Bult CJ. Mouse Genome Informatics (MGI): reflecting on 25 years. *Mamm Genome* 2015;**26**:272–284.

Gao C, Hölscher C, Liu Y, Li L. GSK3: a key target for the development of novel treatments for type 2 diabetes mellitus and Alzheimer disease. *Rev Neurosci* 2011;**23**:1–11.

Gene Ontology Consortium. Gene Ontology Consortium: going forward. *Nucleic Acids Res* 2015;**43**:D1049-56.

Guo TB, Chan KC, Hakovirta H, Xiao Y, Toppari J, Mitchell AP, Salameh WA. Evidence for a role of glycogen synthase kinase-3 beta in rodent spermatogenesis. *J Androl* 2003;**24**:332–342.

Hashemitabar M, Sabbagh S, Orazizadeh M, Ghadiri A, Bahmanzadeh M. A proteomic analysis on human sperm tail: comparison between normozoospermia and asthenozoospermia. *J Assist Reprod Genet* 2015;**32**:853–863.

Hornbeck P V, Zhang B, Murray B, Kornhauser JM, Latham V, Skrzypek E. PhosphoSitePlus, 2014: mutations, PTMs and recalibrations. *Nucleic Acids Res* 2015;**43**:D512-20.

Jing X, Xing R, Zhou Q, Yu Q, Guo W, Chen S, Chu Q, Feng C, Mao X. [Expressions of cysteine-rich secretory protein 2 in asthenospermia]. *Zhonghua Nan Ke Xue* 2011;**17**:203–207.

Kaidanovich-Beilin O, Woodgett JR. GSK-3: Functional Insights from Cell Biology and Animal Models.

Front Mol Neurosci 2011;**4**:40.

Khan Z, Vijayakumar S, la Torre TV de, Rotolo S, Bafico A. Analysis of endogenous LRP6 function reveals a novel feedback mechanism by which Wnt negatively regulates its receptor. *Mol Cell Biol* 2007;**27**:7291–7301.

Koch S, Acebron SP, Herbst J, Hatiboglu G, Niehrs C. Post-transcriptional Wnt Signaling Governs Epididymal Sperm Maturation. *Cell* 2015;**163**:1225–1236.

Li H, Yu N, Zhang X, Jin W, Li H. Spermatozoal protein profiles in male infertility with asthenozoospermia. *Chin Med J (Engl)* 2010;**123**:2879–2882.

Li Y-S, Feng X-X, Ji X-F, Wang Q-X, Gao X-M, Yang X-F, Pan Z-H, Sun L, Ma K. [Expression of SEPT4 protein in the ejaculated sperm of idiopathic asthenozoospermic men]. *Zhonghua Nan Ke Xue* 2011;**17**:699–702.

Logue JS, Whiting JL, Tunquist B, Sacks DB, Langeberg LK, Wordeman L, Scott JD. AKAP220 protein organizes signaling elements that impact cell migration. *J Biol Chem* 2011;**286**:39269–39281.

Niehrs C, Shen J. Regulation of Lrp6 phosphorylation. *Cell Mol Life Sci* 2010;**67**:2551–2562.

Orchard S, Kerrien S, Abbani S, Aranda B, Bhate J, Bidwell S, Bridge A, Briganti L, Brinkman FSL, Brinkman F, *et al.* Protein interaction data curation: the International Molecular Exchange (IMEx) consortium. *Nat Methods* 2012;**9**:345–350.

Organization WH. *Examination and processing of human semen*. *World Health* 2010;**Fifth Edit**:

Pan J-B, Hu S-C, Shi D, Cai M-C, Li Y-B, Zou Q, Ji Z-L. PaGenBase: a pattern gene database for the global and dynamic understanding of gene function. *PLoS One* 2013;**8**:e80747.

Petryszak R, Burdett T, Fiorelli B, Fonseca NA, Gonzalez-Porta M, Hastings E, Huber W, Jupp S, Keays M, Kryvych N, *et al.* Expression Atlas update--a database of gene and transcript expression from microarray- and sequencing-based functional genomics experiments. *Nucleic Acids Res*

2014;**42**:D926-32.

Piñero J, Bravo À, Queralt-Rosinach N, Gutiérrez-Sacristán A, Deu-Pons J, Centeno E, García-García J, Sanz F, Furlong LI. DisGeNET: a comprehensive platform integrating information on human disease-associated genes and variants. *Nucleic Acids Res* 2017;**45**:D833–D839.

Pontius JU, Wagner L, Schuler GD. UniGene: a unified view of the transcriptome. *NCBI Handb* 2003;**1**:, p. 1–12.

Pronobis MI, Rusan NM, Peifer M. A novel GSK3-regulated APC:Axin interaction regulates Wnt signaling by driving a catalytic cycle of efficient βcatenin destruction. *Elife* 2015;**4**:e08022.

Reinton N, Collas P, Haugen TB, Skâlhegg BS, Hansson V, Jahnsen T, Taskén K. Localization of a novel human A-kinase-anchoring protein, hAKAP220, during spermatogenesis. *Dev Biol* 2000;**223**:194–204.

Salvolini E, Buldreghini E, Lucarini G, Vignini A, Giulietti A, Lenzi A, Mazzanti L, Primio R Di, Balercia G. Interleukin-1β, cyclooxygenase-2, and hypoxia-inducible factor-1α in asthenozoospermia. *Histochem Cell Biol* 2014;**142**:569–575.

Saraswat M, Joenväärä S, Jain T, Tomar AK, Sinha A, Singh S, Yadav S, Renkonen R. Human Spermatozoa Quantitative Proteomic Signature Classifies Normo- and Asthenozoospermia. *Mol Cell Proteomics* 2017;**16**:57–72.

Schimenti KJ, Feuer SK, Griffin LB, Graham NR, Bovet CA, Hartford S, Pendola J, Lessard C, Schimenti JC, Ward JO. AKAP9 is essential for spermatogenesis and sertoli cell maturation in mice. *Genetics* 2013;**194**:447–457.

Shannon P, Markiel A, Ozier O, Baliga NS, Wang JT, Ramage D, Amin N, Schwikowski B, Ideker T. Cytoscape: a software environment for integrated models of biomolecular interaction networks. *Genome Res* 2003;**13**:2498–2504.

Shen C, Kuang Y, Liu J, Feng J, Chen X, Wu W, Chi J, Tang L, Wang Y, Fei J, *et al.* Prss37 is required for male fertility in the mouse. *Biol Reprod* 2013a;**88**:123.

Shen S, Wang J, Liang J, He D. Comparative proteomic study between human normal motility sperm and idiopathic asthenozoospermia. *World J Urol* 2013b;**31**:1395–1401.

Smith GD, Wolf DP, Trautman KC, Cruz e Silva EF da, Greengard P, Vijayaraghavan S. Primate sperm contain protein phosphatase 1, a biochemical mediator of motility. *Biol Reprod* 1996;**54**:719–727.

Smith GD, Wolf DP, Trautman KC, Vijayaraghavan S. Motility potential of macaque epididymal sperm: the role of protein phosphatase and glycogen synthase kinase-3 activities. *J Androl* 1999;**20**:47–53.

Somanath PR, Jack SL, Vijayaraghavan S. Changes in sperm glycogen synthase kinase-3 serine phosphorylation and activity accompany motility initiation and stimulation. *J Androl***25**:605–617.

Song X, Wang S, Li L. New insights into the regulation of Axin function in canonical Wnt signaling pathway. *Protein Cell* 2014;**5**:186–193.

Stamos JL, Weis WI. The β-catenin destruction complex. *Cold Spring Harb Perspect Biol* 2013;**5**:a007898.

Tanji C, Yamamoto H, Yorioka N, Kohno N, Kikuchi K, Kikuchi A. A-kinase anchoring protein AKAP220 binds to glycogen synthase kinase-3beta (GSK-3beta) and mediates protein kinase A-dependent inhibition of GSK-3beta. *J Biol Chem* 2002;**277**:36955–36961.

Tyanova S, Temu T, Sinitcyn P, Carlson A, Hein MY, Geiger T, Mann M, Cox J. The Perseus computational platform for comprehensive analysis of (prote)omics data. *Nat Methods* 2016;**13**:731–740.

Uhlén M, Fagerberg L, Hallström BM, Lindskog C, Oksvold P, Mardinoglu A, Sivertsson Å, Kampf C, Sjöstedt E, Asplund A, *et al.* Proteomics. Tissue-based map of the human proteome. *Science* 2015;**347**:1260419.

Varmuza S, Jurisicova A, Okano K, Hudson J, Boekelheide K, Shipp EB. Spermiogenesis is impaired in mice bearing a targeted mutation in the protein phosphatase 1cgamma gene. *Dev Biol* 1999;**205**:98–110.

Vijayaraghavan S, Mohan J, Gray H, Khatra B, Carr DW. A role for phosphorylation of glycogen synthase kinase-3alpha in bovine sperm motility regulation. *Biol Reprod* 2000;**62**:1647–1654.

Vijayaraghavan S, Stephens DT, Trautman K, Smith GD, Khatra B, Cruz e Silva EF da, Greengard P. Sperm motility development in the epididymis is associated with decreased glycogen synthase kinase-3 and protein phosphatase 1 activity. *Biol Reprod* 1996;**54**:709–718.

Voronkov A, Krauss S. Wnt/beta-catenin signaling and small molecule inhibitors. *Curr Pharm Des* 2013;**19**:634–664.

Wang QM, Fiol CJ, DePaoli-Roach AA, Roach PJ. Glycogen synthase kinase-3 beta is a dual specificity kinase differentially regulated by tyrosine and serine/threonine phosphorylation. *J Biol Chem* 1994;**269**:14566–14574.

Wang R-S, Yeh S, Tzeng C-R, Chang C. Androgen receptor roles in spermatogenesis and fertility: lessons from testicular cell-specific androgen receptor knockout mice. *Endocr Rev* 2009;**30**:119–132.

Wu C, Jin X, Tsueng G, Afrasiabi C, Su AI. BioGPS: building your own mash-up of gene annotations and expression profiles. *Nucleic Acids Res* 2016;**44**:D313-6.

Wu G, Huang H, Garcia Abreu J, He X. Inhibition of GSK3 phosphorylation of beta-catenin via phosphorylated PPPSPXS motifs of Wnt coreceptor LRP6. *PLoS One* 2009;**4**:e4926.

Xue Y, Liu Z, Cao J, Ma Q, Gao X, Wang Q, Jin C, Zhou Y, Wen L, Ren J. GPS 2.1: enhanced prediction of kinase-specific phosphorylation sites with an algorithm of motif length selection. *Protein Eng Des Sel* 2011;**24**:255–260.

Yu W, Clyne M, Khoury MJ, Gwinn M. Phenopedia and Genopedia: disease-centered and gene-centered views of the evolving knowledge of human genetic associations. *Bioinformatics* 2010;**26**:145–146.

Zeidner LC, Buescher JL, Phiel CJ. A novel interaction between Glycogen Synthase Kinase-3α (GSK-3α) and the scaffold protein Receptor for Activated C-Kinase 1 (RACK1) regulates the circadian clock. *Int J Biochem Mol Biol* 2011;**2**:318–327.

Zeng X, Tamai K, Doble B, Li S, Huang H, Habas R, Okamura H, Woodgett J, He X. A dual-kinase mechanism for Wnt co-receptor phosphorylation and activation. *Nature* 2005;**438**:873–877.

Zhou J-H, Zhou Q-Z, Lyu X-M, Zhu T, Chen Z-J, Chen M-K, Xia H, Wang C-Y, Qi T, Li X, *et al.* The expression of cysteine-rich secretory protein 2 (CRISP2) and its specific regulator miR-27b in the spermatozoa of patients with asthenozoospermia. *Biol Reprod* 2015;**92**:28.

Captation Supplementary Data

Supplementary Figure 1. Expression and auto-activation of the reporter genes tests of pAS2-1-GSK3A and pAS2-1-GSK3B in AH190 yeasts. A. Yeast protein extracts previously transformed with pAS2-1-GSK3A or pAS2-1-GSK3B were probed with an anti-GSK3B antibody (Cell Signaling ref:#9338,1:1000) and an anti- GSK3B antibody (Cell Signaling ref: #9315, 1:1000). The calculated molecular weight of hybrid protein is presented. B. Yeast transformed with pAS2-1; pAS2-1-GSK3A or pAS2-1-GSK3B were plated in different levels of stringency mediums.

Supplementary Figure 2. Solubilizing effect of different lysis buffers for GSK3A and GSK3B. A. 1% SDS is very effective on solubilizing GSK3. For GSK3A, 1XRIPA and 1XRIPA modified solubilized approximately half of the protein and 20mM Tris-HCl only 30%, when compared with 1%SDS. For GSK3B, 1xRIPA and 1XRIPA modified solubilized around 70% of GSK3B and 20mM of Tris-HCl only30%, when compared with 1%SDS. GSK3A and GSK3B were detected using an anti-GSK3A/B (Invitrogen, ref: 44-610, 1:2000).

Supplementary Figure 3. Co-Immunoprecipitation of GSK3 from normospermic human spermatozoa sample. Both co-immunoprecipitations were also used for identification of GSK3 interactors by mass spectrometry. GSK3A and GSK3B were detected using an anti-GSK3A/B (Invitrogen, ref: 44-610, 1:2000). A. After co-immunoprecipitation with either a GSK3A or GSK3B specific antibody, proteins were eluted with 1% SDS or 50mM glycine. B. After co-immunoprecipitation with crosslink of GSK3A or GSK3B antibodies to dynabeads beads, 1⁄4 of the beads were eluted with 1%SDS and GSK3A or GSK3B presence was evaluated. C. Prior to GSK3 immunodetection, APP presence was evaluated by probing with 6E10 antibody. Although the reason is unknown, upon incubation with the 6E10 antibody (Sigma-Aldrich, ref: A-1474), two unspecific bands appear on the negative control eluted with 50mM of glycine.

Supplementary Figure 4. GSK3A-centred protein-protein interactome network. All GSK3A interactors (testis, sperm and databased) were used to build the network. Node size: degree (number of neighbors of a protein).

Supplementary Figure 5. GSK3B-centred protein-protein interactome network. All GSK3B interactors (testis, sperm and databased) were used to build the network. Node size: degree (number of neighbors of a protein).

Supplementary Figure 6. GSK3-centered subnetwork for male infertility annotations extracted from GSK3 interactome network. GSK3 interactors associated with male infertility annotations were used to build the network. Solid lines: testis or sperm GSK3 interactions; Dashed lines: Databased retrieved GSK3 interactions. Node size: according to testis expression. Node colors: represent male infertility related phenotypes, biological processes (BP) or cellular components (CC).

Supplementary Table I. Characterization of human sperm samples used for GSK3 analysis in normospermic and asthenozoospermic samples.

Supplementary Table II: Correlation coefficient between % of immotile, progressive motility and progressive motility + non-progressive motility sperm and total and serine phosphorylated GSK3 in human sperm samples.

Supplementary Table III: GSK3α human testis interactors. Gene name, UniProtKB, nr of clones, GSK3 phosphorylation site, previously described GSK3 interactor, presence on mammalian testis and sperm, alteration on asthenozoospermic samples and tissue expression (HPA RNA expression) of testis GSK3α interactors. Mixed expression is defined as being expressed in at least one tissue but in neither ubiquitous or tissue-enriched. *Although RNA expression described for HMBS is enriched for bone-marrow, protein expression reveals that is expressed in several tissues.

Supplementary Table IV. GSK3B human testis interactors. Gene name, UniProtKB, nr of clones, GSK3 phosphorylation site, previously described GSK3 interactor, presence on mammalian testis and sperm and alteration on asthenozoospermic samples and tissue expression (HPA RNA expression) of testis GSK3B interactors. Mixed expression is defined as being expressed in at least one tissue but in neither ubiquitous or tissue-enriched.

Supplementary Table V. GSK3 isoforms peptides detected on mass spectrometry. Peptide sequence, first and last aminoacid of the peptide, peptide % of coverage for the complete protein and peptide spectral count.

Supplementary Table VI. GSK3A human sperm interactors. Gene name, UniProtKB, nr of clones, GSK3 phosphorylation site, previously described GSK3 interactor, presence on mammalian testis and sperm and alteration on asthenozoospermic samples and tissue expression (HPA RNA expression) of testis GSK3A interactors. Mixed expression is defined as being expressed in at least one tissue but in neither ubiquitous or tissue-enriched.

Supplementary Table VII. GSK3B human sperm interactors. Gene name, UniProtKB, mass spectrometry score, GSK3 phosphorylation site, previously described GSK3 interactor, presence on mammalian testis and sperm, alteration on asthenozoospermic samples and tissue expression (HPA RNA expression) of sperm GSK3b interactors.

Supplementary Table VIII. Testis expression levels of GSK3A interactome. Expression levels of all GSK3 interactors were retrieved form the Human Protein Atlas, PaGeneBase, Expression atlas, BioGPS and UniGene. Testis expression values were normalized. Yellow: GSK3A testis interactors; Green: GSK3A sperm interactors; Orange: GSK3A database interactors.

Supplementary Table IX: Testis expression levels of GSK3B interactome. Expression levels of all GSK3 interactors were retrieved form the human protein atlas, PaGeneBase, Expression atlas, BioGPS and UniGene were retrieved and testis expression values were normalized. Yellow: GSK3B testis interactors; Green: GSK3B sperm interactors; Orange: GSK3B database interactors.

Supplementary Table X. Testis enriched GSK3 interactors. To be classified as testis enriched, expression must be > 50% in testis in at least 2 databases. Interactors were classified in three categories: 50-75%; 75%-90 and >90%.

Supplementary Table XI. Testis and sperm related phenotypes/diseases/annotations of GSK3A interactome. Testis and sperm related phenotypes/diseases/annotations of all GSK3A interactors were retrieved and categorized. Yellow: GSK3A testis interactors; Green: GSK3A sperm interactors; Orange: GSK3α database interactors.

Supplementary Table XII. Testis and sperm related phenotypes/diseases/annotations of GSK3B interactome. Testis and sperm related phenotypes/diseases/annotations of all GSK3B interactors were retrieved and categorized. Yellow: GSK3B testis interactors; Green: GSK3B sperm interactors; Orange: GSK3B database interactors.

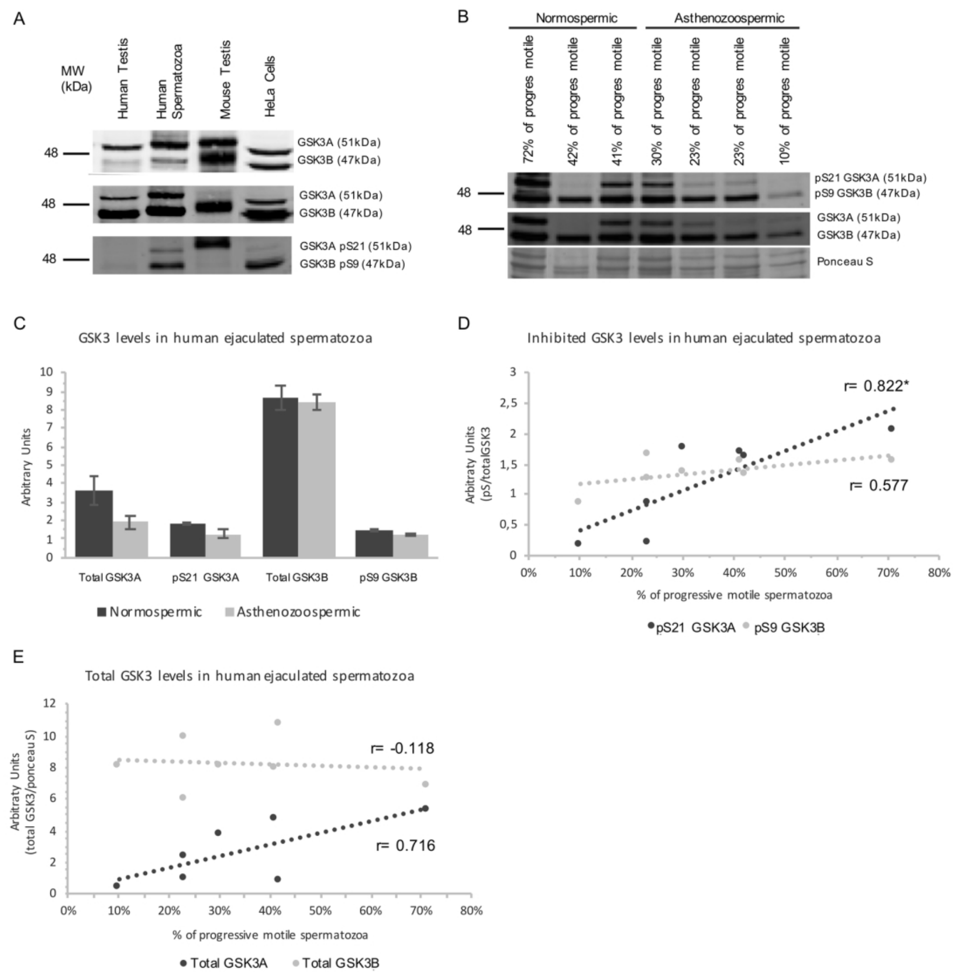

Figure 1. GSK3 in human testis and spermatozoa and correlation with sperm motility. A. Western blot analysis of total GSK3 and serine phosphorylated GSK3 isoforms in human testis and spermatozoa, mouse testis and HeLa cells. 30µg of protein obtained in RIPA1x were loaded per sample. From up to down GSK3 was immunodetected with the following antibodies: anti-GSK3A/B antibody; anti-GSK3A antibody and anti-GSK3B antibody; anti-GSK3A pS21 and anti-GSK3B pS9 B. Immunoblot of total and serine phosphorylated GSK3 isoforms in human normospermic (n=3) and asthenozoospermic (n=4) ejaculated spermatozoa. C. Total and serine phosphorylated GSK3 isoforms protein levels in human normospermic and asthenozoospermic (bar chart with error bars (SEM)). D. Pearson Correlation between the percentage of progressive motile ejaculated sperm and protein levels of serine phosphorylated GSK3A and GSK3B (scatter plot with regression line). E. Pearson Correlation between the percentage of progressive motile ejaculated sperm and protein levels of total GSK3A and GSK3B. Blots were cropped. * Correlation is statistically significant at the 0.05 level

159x162mm (300 x 300 DPI)

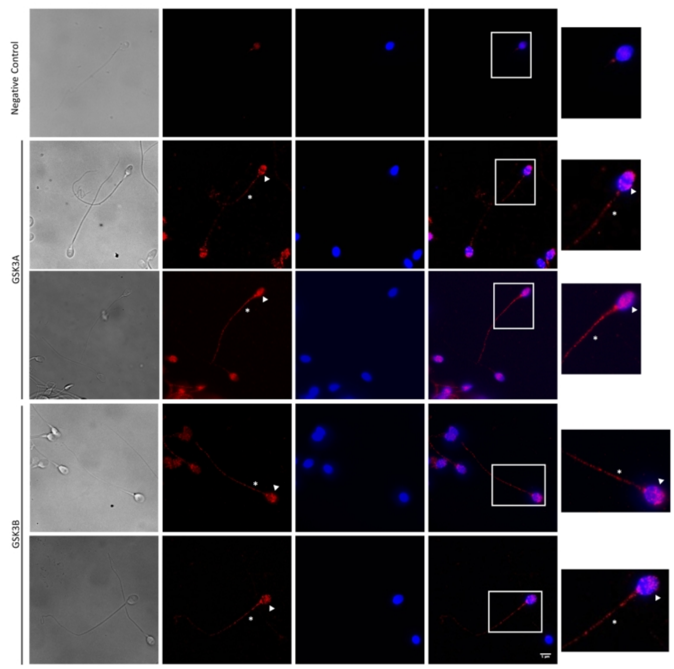

Figure 2. Subcelular localization of GSK3A and GSK3B in normospermic ejaculated human sperm. GSK3A is located in the flagellum (star) and head (arrowhead), more specifically in the equatorial region. GSK3B is located through the entire head (arrowhead) and occasionally in the flagellum (star). 100 sperm cells were counted per samples. Experiment done in triplicate. Scale bar is 5 μm. Nucleus is marked in blue. ROI: region of interest. All images were obtained with 63X magnification.

190x275mm (300 x 300 DPI)

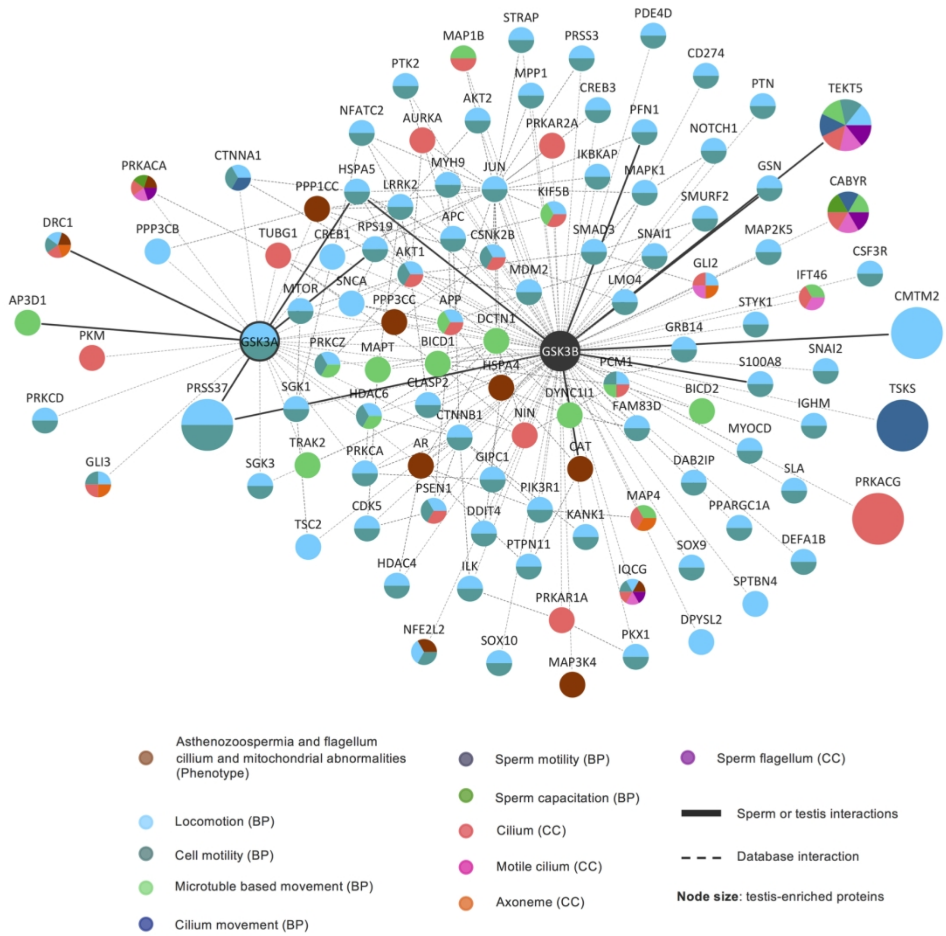

Figure 3. GSK3-centered subnetwork for sperm motility extracted from GSK3 interactome network. All GSK3 interactors associated with motility-related annotations were used to build the network. Solid lines: testis or sperm GSK3 interactions; Dashed lines: Databased-retrieved GSK3 interactions. Node size: according to testis expression. Node colors: represent motility-related phenotypes, biological processes (BP) or cellular components (CC).

166x157mm (300 x 300 DPI)

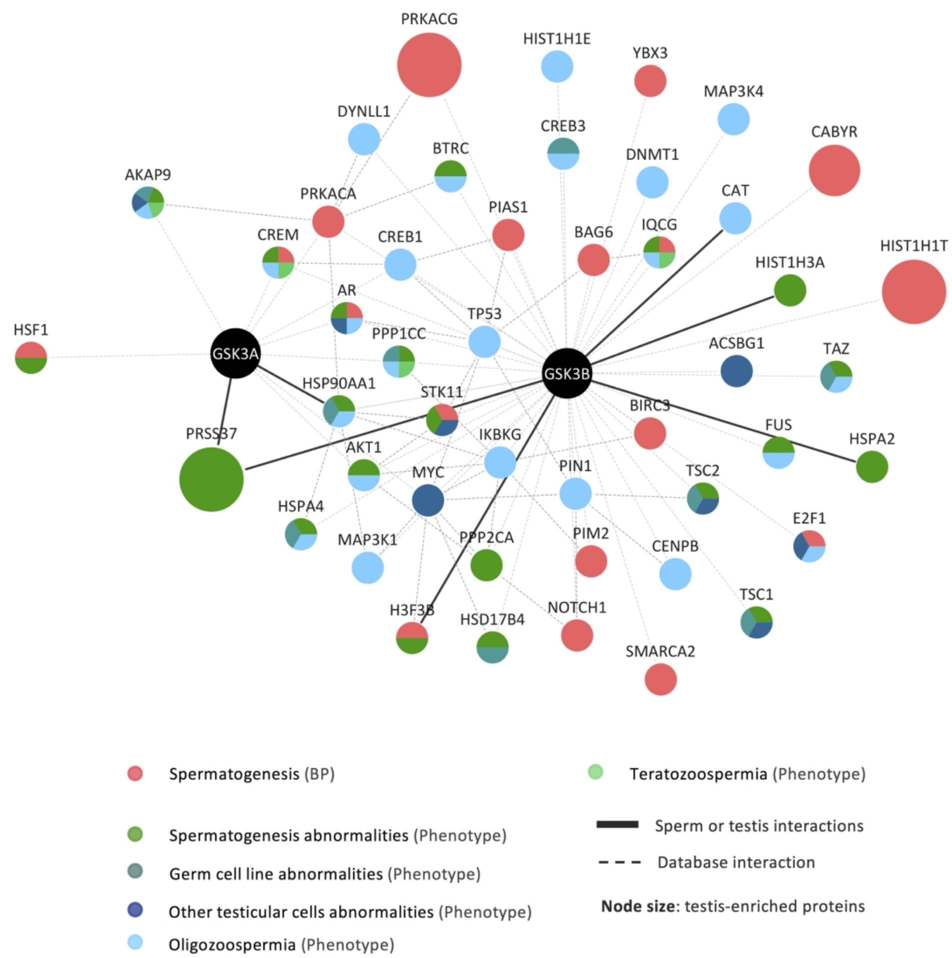

Figure 4. GSK3-centered subnetwork for testis-related annotations extracted from GSK3 interactome network. All GSK3 interactors associated with testis annotations were used to build the network. Solid lines: testis or sperm GSK3 interactions; Dashed lines: Databased retrieved GSK3 interactions. Node size: according to testis expression. Node colours: represent testis related phenotypes, biological processes (BP) or cellular components (CC).

158x160mm (300 x 300 DPI)

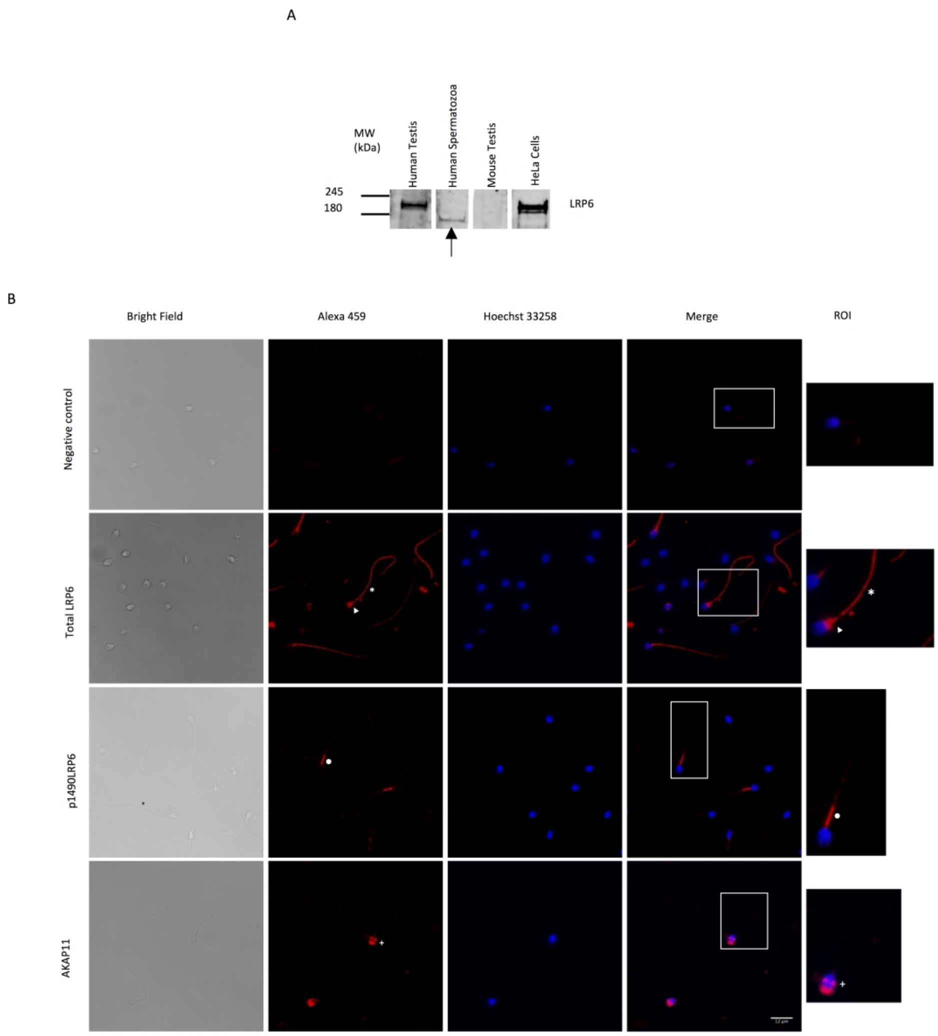

Figure 5. LRP6 and AKAP11 in human testis and ejaculated normospermic sperm. A. Western blot analysis of LRP6 in human testis and ejaculated sperm, mouse testis and HeLa cells. For human testis, mouse testis and HeLa cells 30µg of protein were loaded per sample. For ejaculated human sperm 100µg of proteins were loaded. Note according to the antibody datasheet that the antibody only recognizes human and rat LRP6. Arrow highlights the LRP6 presence in human sperm. B. Subcellular localization of LRP6, p1490LRP6 and AKAP11 in mature human sperm. Total LRP6 is located in the entire flagellum (star) and occasionally in the post-acrosomal area (arrowhead). The phosphorylated form of LRP6 at serine 1490 is restricted to the midpiece (circle). AKAP11 is located to the head, specifically to the anterior and equatorial area (plus sign). Blots were cropped. 100 sperm cells were counted per samples. Experiment done in triplicate. Scale bar is 10µm. Nucleus is marked in blue. ROI: region of interest. All images were obtained with 63X magnification.

1523x1702mm (72 x 72 DPI)

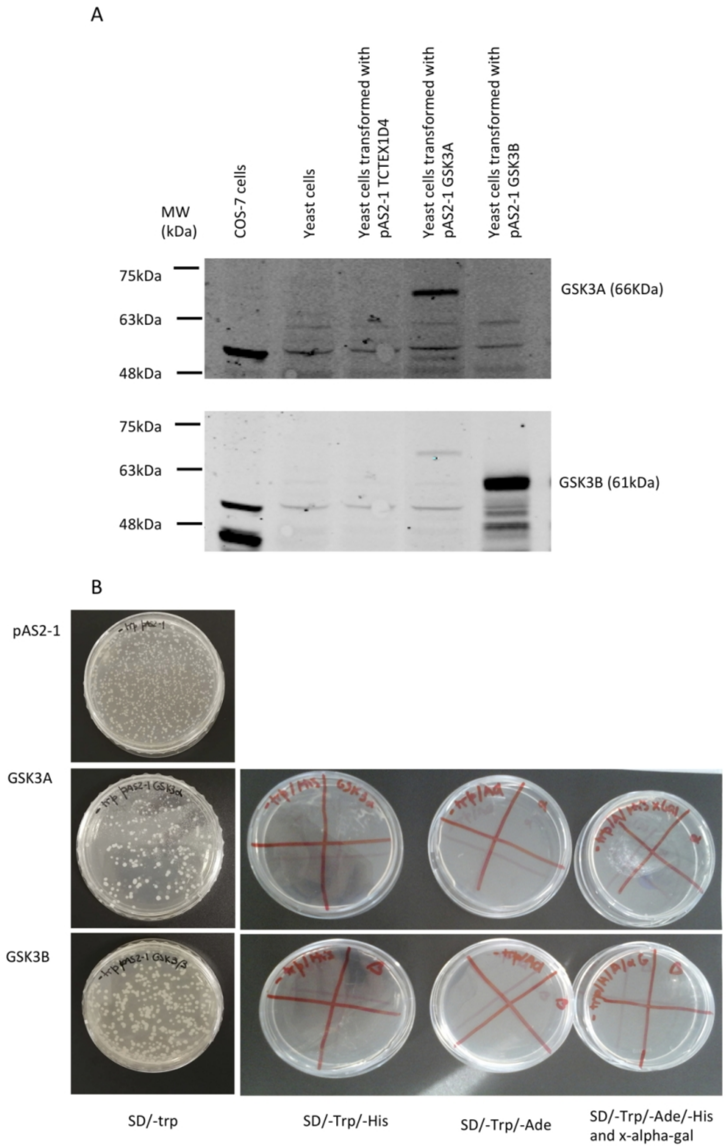

102x152mm (300 x 300 DPI)

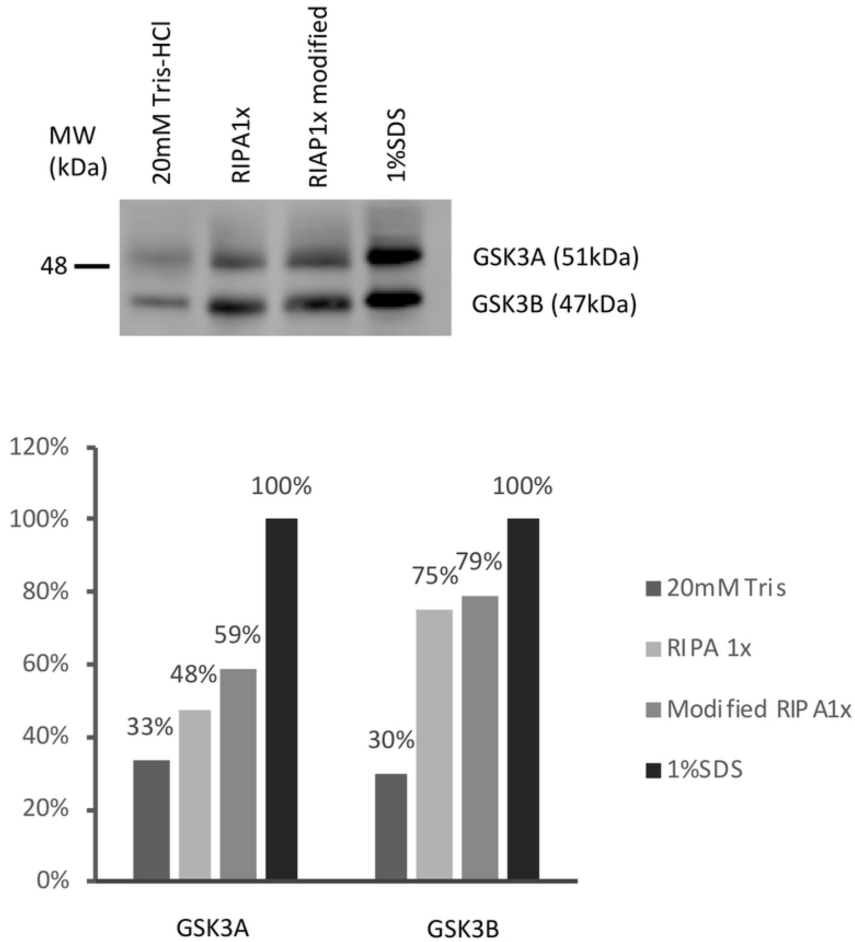

77x82mm (300 x 300 DPI)

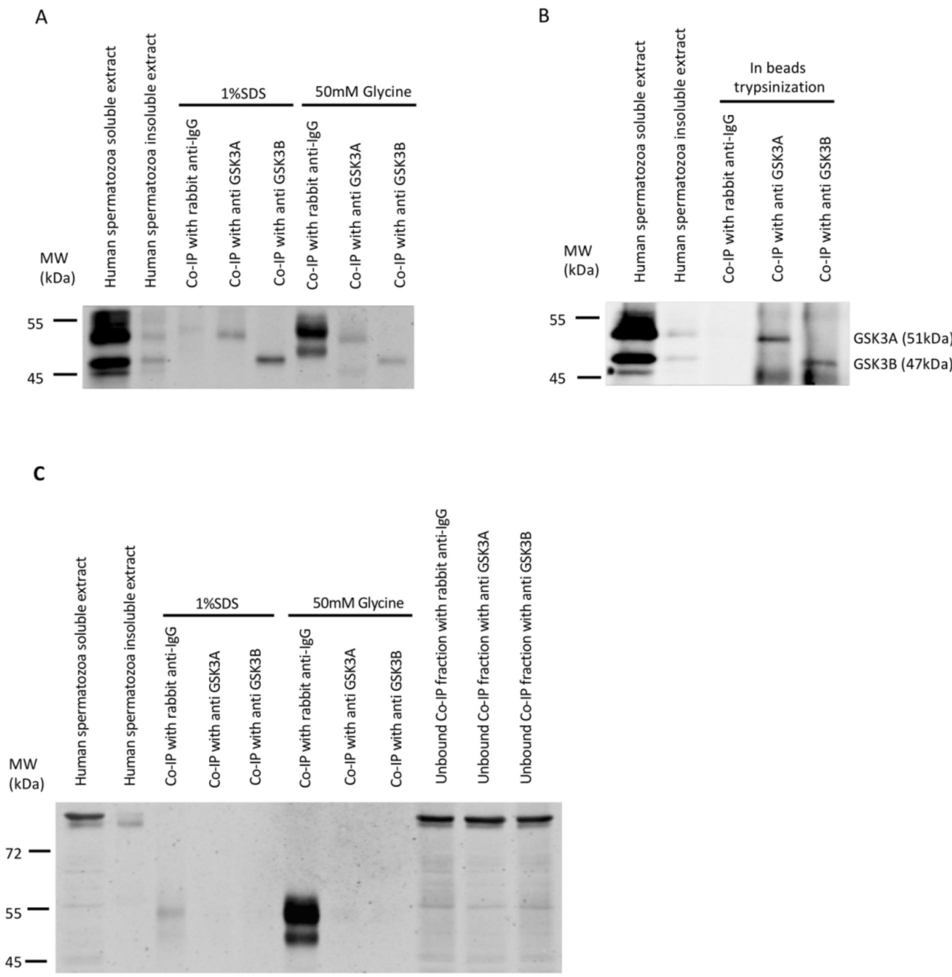

128x132mm (300 x 300 DPI)

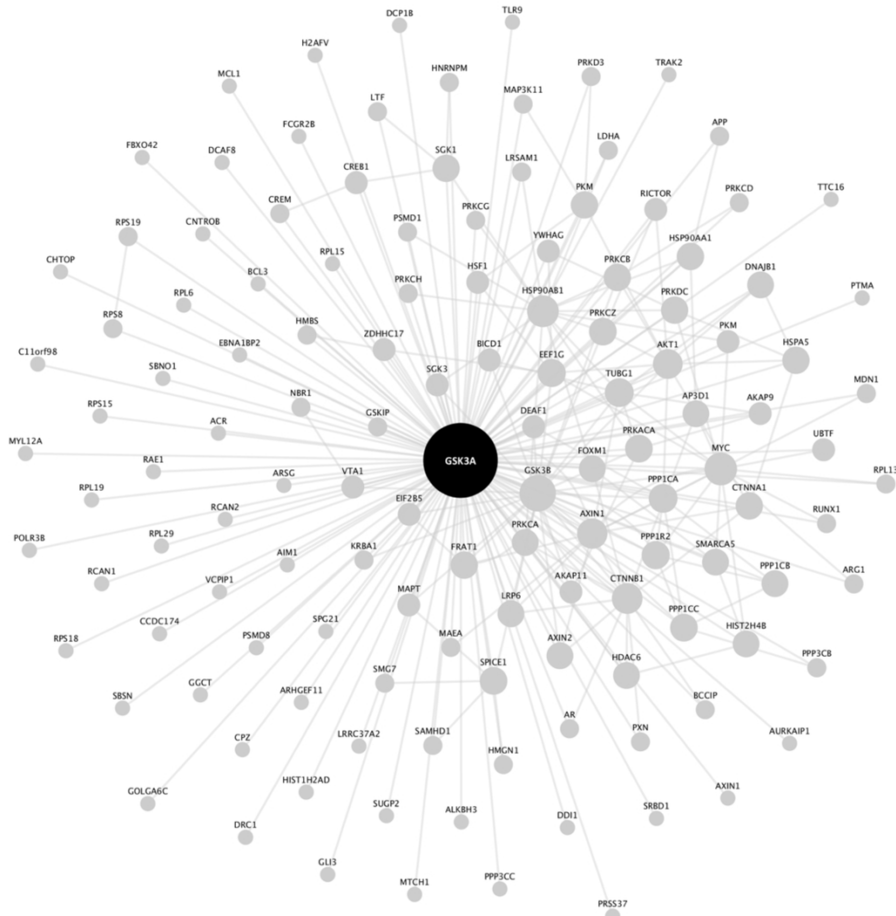

109x109mm (300 x 300 DPI)

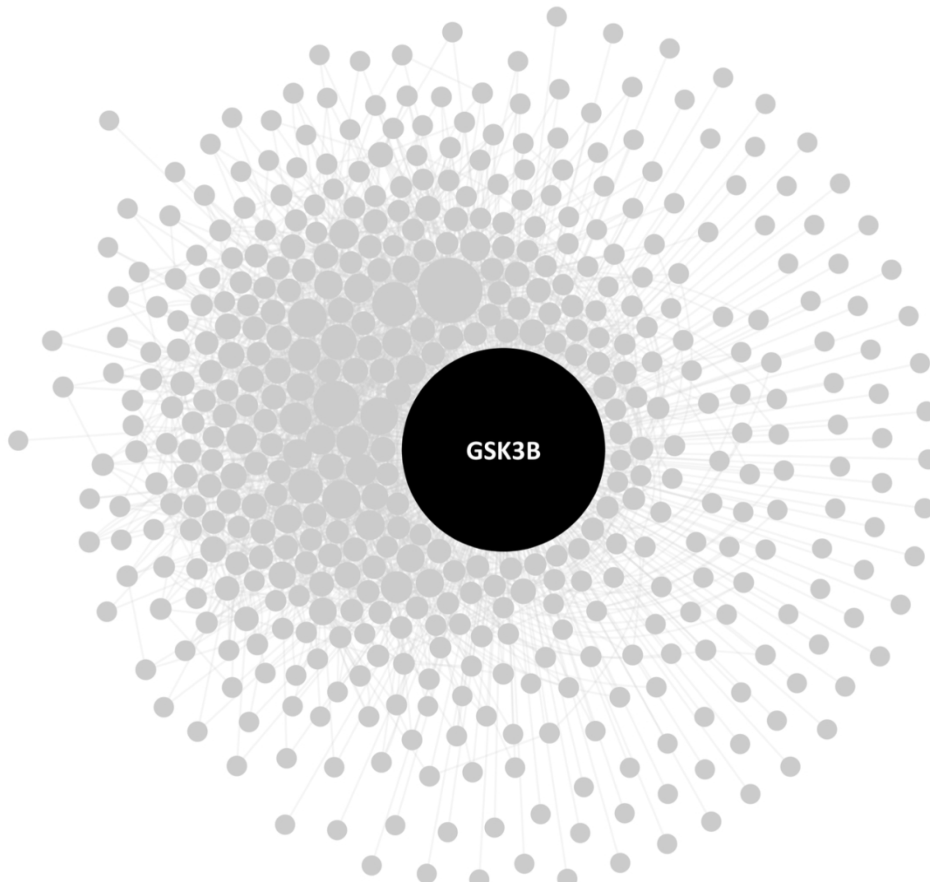

115x106mm (300 x 300 DPI)

Supplementary Table I. Characterization of human sperm samples used for GSK3 a

Samples	Volume (ml)	Concentration (million/mL)	Progressive (%)
32-000252	2	300	71
32-000309	4.8	80	42
32-000255	4	85	41
32-000335	3.5	229	30
32-000307	4.3	24	23
32-000310	4	130	23
10309	4	20	10

Lower references of normospermic samples classification criteria according to WHO
Volume: 1.5mL
Concentration: 15x106/mL or 39x106/ejaculate
Motility:
Progressive+non-progressive: 40%
Progressive: 32%
Morphology: 4%

ınalysis in normospermic and asthenozoospermic samples

Motility		Morphology (%)
Non-progressive (%)	Immotile (%)	Normal
7	22	14
19	39	9
10	49	8
14	56	12
18	59	8
5	72	8
15	75	1

ı laboratory manual for the Examination and processing of human semen, fifth edition

Supplementary Table II: Correlation coefficient between % of immotile, progressi

% Immotile sperm

**. Correlation is significant at the 0.01 level (2-tailed); very strong (negative)

% Progressive motility

*. Correlation is significant at the 0.05 level (2-tailed); very strong (positive)

% Progressive motility+non progressive motility

**. Correlation is significant at the 0.01 level (2-tailed)¸very strong (positive)

ive motility and progressive motility+non progresive motility sperm and total and serine

	Total GSK3α	pS21 GSK3α	Total GSK3β	pS9 GSK3β
Pearson Correlation	-,648	-,878**	-,149	-,418
Sig. (2-tailed)	,116	,009	,750	,351
N	7	7	7	7

	Total GSK3α	pS21 GSK3α	Total GSK3β	pS9 GSK3β
Pearson Correlation	,716	,822*	-,118	,577
Sig. (2-tailed)	,070	,023	,801	,175
N	7	7	7	7

	Total GSK3α	pS21 GSK3α	Total GSK3β	pS9 GSK3β
Pearson Correlation	,652	,885**	,190	,374
Sig. (2-tailed)	,113	,008	,684	,408
N	7	7	7	7

phosphorylated GSK3 in human sperm samples.

Supplementary Table III

Gene Name	UniProtKB
AKAP11	Q9UKA4
ALKBH3	Q96Q83
AP3D1	O14617
AURKAIP1	Q9NWT8
AXIN2	Q9Y2T1
BCCIP	Q9P287
C11orf98	E9PRG8
CCDC174	Q6PII3
CHTOP	Q9Y3Y2
CNTROB	Q8N137
DCAF8	Q5TAQ9
DCP1B	Q8IZD4
DDI1	Q8WTU0
DEAF1	O75398
DNAJB1	P25685
DRC1	Q96MC2
FBXO42	Q6P3S6
GOLGA6C	A6NDK9
H2AFV	Q71UI9
HMBS	P08397
HMGN1	P05114
HNRNPM	P52272
HSP90AA1	P07900
HSP90AB1	P08238
LDHA	P00338
LRP6	O75581
LRRC37A2	A6NM11
MAEA	Q7L5Y9
MTCH1	Q9NZJ7
MYL12A	P19105
NBR1	Q14596
PSMD8	P48556
PTMA	P06454
RPL15	P61313
RPL19	P84098
RPL29	P47914
RPS15	P62841
RPS19	P39019
RUNX1	Q01196
SBNO1	A3KN83
SMARCA5	O60264
SMG7	Q92540
SUGP2	Q8IX01

TTC16	Q8NEE8
UBTF	P17480
VCPIP1	Q96JH7
Homo Sapiens Chromosor	
Human Dna sequence fro	
RefSeqGene on chromoso	

l: GSK3α human testis interactors. Gene name, UniProtKB, nr of clones, GSK3 phosphorylatic

Name
A-kinase anchor protein 11
Alpha-ketoglutarate-dependent dioxygenase alkB homolog 3
AP-3 complex subunit delta-1
Aurora kinase A-interacting protein
Axin-2
BRCA2 and CDKN1A-interacting protein
Uncharacterized protein C11orf98
Coiled-coil domain-containing protein 174
Chromatin target of PRMT1 protein
Centrobin
DDB1- and CUL4-associated factor 8
mRNA-decapping enzyme 1B
Protein DDI1 homolog 1
Deformed epidermal autoregulatory factor 1 homolog
DnaJ homolog subfamily B member 1
Dynein regulatory complex protein 1
F-box only protein 42
Golgin subfamily A member 6C
Histone H2A.V
Porphobilinogen deaminase
Non-histone chromosomal protein HMG-14
Heterogeneous nuclear ribonucleoprotein M
Heat shock protein HSP 90-alpha
Heat shock protein HSP 90-beta
L-lactate dehydrogenase A chain
Low-density lipoprotein receptor-related protein 6
Leucine-rich repeat-containing protein 37A2
Macrophage erythroblast attacher
Mitochondrial carrier homolog 1
Myosin regulatory light chain 12A
Next to BRCA1 gene 1 protein
26S proteasome non-ATPase regulatory subunit 8
Prothymosin alpha
60S ribosomal protein L15
60S ribosomal protein L19
60S ribosomal protein L29
40S ribosomal protein S15
40S ribosomal protein S19
Runt-related transcription factor 1
Protein strawberry notch homolog 1
SWI/SNF-related matrix-associated actin-dependent regulator of chromatin subfamily A member 5
Protein SMG7
SURP and G-patch domain-containing protein 2

Tetratricopeptide repeat protein 16
Nucleolar transcription factor 1
Deubiquitinating protein VCIP135
me 21 clone CTD-250 3J9 map p11-q21.1
m clone RP11-543N17
ome 5 Chromosome 5: 150,401,911-150,402,122

:e, previously described GSK3 interactoı

Nr of clones	GSK3 phosphorylation site
1	Yes
1	
1	Yes
2	Yes
1	Yes
7	Yes
1	
1	Yes
1	
1	Yes
1	Yes
5	Yes
1	Yes
1	Yes
1	
1	Yes
1	Yes
1	
1	
1	
1	
1	
12	Yes
4	
1	
1	Yes
1	Yes
1	Yes
1	Yes
1	
1	Yes
3	
2	
1	
1	
1	
1	
1	
1	Yes
2	Yes
1	Yes
1	Yes
1	Yes

1 Yes
1 Yes
1 Yes
1
1
2

r, presence on mammalian testis and sperm, alteration on asthenozoospermic samples and tis

Previously known GSK3 interactor (DOI or PMID)
GSK3β [10.1074/jbc.M206210200]
GSK3α and GSK3β [10.1016/j.celrep.2013.03.027] [10.1038/nmeth.2400] [10.1038/79039] [1
GSK3α and GSK3β [10.1074/mcp.M900568-MCP200]
GSK3α and GSK3β [10.1038/nmeth.2400] [10.1016/j.cell.2012.06.047] [10.1038/onc.2012.31
GSK3α and GSK3β [10.1038/nmeth.2400] [10.1016/j.cell.2012.06.047] [10.1038/onc.2012.31
GSK3α and GSK3β [10.1074/jbc.M508657200] [10.1016/j.devcel.2006.07.003]
GSK3α and GSK3β [10.1074/mcp.M900568-MCP200] [10.4161/auto.28479]
GSK3β [10.1038/nmeth.2400]
GSK3β [10.1038/nmeth.2400]
GSK3β [10.1038/nmeth.2400]
GSK3β [10.1038/nmeth.2400]

(HPA RNA expression) of testis GSK3α interactors. Mixed expression is defined as being expr

Present in testis and/or sperm (DOI or PMID)
Human testis and human sperm [10.1006/dbio.2000.9725]
Mouse testis [10.1073/pnas.1601461113]
Mouse testis (spermatocyte and spermatids) [10.1095/biolreprod.109.078980]
Human sperm (midpiece and principle piece) [10.1038/nrurol.2016.89]
Mouse testis and human sperm (mRNA) [10.1371/journal.pgen.1004825] [10.1371/journal.pone.012
Mouse testis (mRNA) and human sperm [10.1177/1933719112452939] [10.1371/journal.pone.0115ℇ
Rat testis (Sertoli cells) and human sperm (equatorial region) note that does not distinct AA1 from AB
Human sperm (principal piece) [https://doi.org/10.1095/biolreprod32.5.1201]
Human sperm (flagellum more intense in midpiece) [10.1016/j.cell.2015.10.029]
Human testis (mRNA) [https://doi.org/10.1016/S0378-1119(00)00549-7]
Boar sperm (acrosome) [10.1016/j.jri.2009.11.002]
Rat testis (Leydig cells, panchytene spermatocyte and spermatids) and human sperm (acrosome) [10.
Human sperm [10.1371/journal.pone.0127007]
Mouse testis [10.4103/1008-682X.133318]
Mouse testis [10.1016/j.jmb.2011.11.041]
Mouse testis (spermatocytes and spermatids) [10.1371/journal.pgen.1005863]

one tissue but in neither ubiquitous or tissue-enriched. *Although RNA expression

Asthenozoospermic alteration (DOI or PMID)	Tissue expression (HPA)
	Ubiquitous
	Ubiquitous
	Ubiquitous
	Ubiquitous
	Mixed
	Ubiquitous
	Ubiquitous
	Ubiquitous
	Ubiquitous
	Ubiquitous
	Ubiquitous
	Ubiquitous
	Testis-enriched
	Ubiquitous
Upregulated [10.1074/mcp.M116.061028]	Ubiquitous
	Group enriched (testis, epididymis and fa
	Ubiquitous
	Testis-enriched
	Ubiquitous
	Bone marrow-enriched*
	Ubiquitous
	Ubiquitous
Upregulated [10.1074/mcp.M116.061028]	Ubiquitous
Upregulated [10.1074/mcp.M116.061028]	Ubiquitous
Downregulated[36]	Ubiquitous
	Mixed
Upregulated [10.1074/mcp.M116.061028]	Testis-enriched
	Ubiquitous
	Ubiquitous
	Ubiquitous
	Ubiquitous
	Ubiquitous
0.1002/jcp.24332]	Ubiquitous
	Ubiquitous
	Ubiquitous
	Ubiquitous
	Ubiquitous
	Ubiquitous
	Mixed
	Ubiquitous
	Ubiquitous
	Ubiquitous
	Ubiquitous

Group enriched (testis and fallopian tube
Ubiquitous
Mixed

described for HMBS is enriched for bone-marrow, protein expression reveals

allopian tube)

e)

Supplementary Table IV. GSK3β human testis interactors. Gene name, UniProtKB, nr of clones, (

Gene Name	UniProtKB	Name
AXIN2	Q9Y2T1	Axin-2
BCCIP	Q9P287	BRCA2 and CDKN1A-interacting protein
C10orf90	Q96M02	Centrosomal protein C10orf90
C11orf98	E9PRG8	Uncharacterized protein C11orf98
CASC4	Q6P4E1	Protein CASC4
CMTM2	Q8TAZ6	CKLF-like MARVEL transmembrane domain-containing protein 2
DCP1B	Q8IZD4	mRNA-decapping enzyme 1B
HNRNPM	P52272	Heterogeneous nuclear ribonucleoprotein M
HSP90AA1	P07900	Heat shock protein HSP 90-alpha
HSP90AB1	P08238	Heat shock protein HSP 90-beta
LYAR	Q9NX58	Cell growth-regulating nucleolar protein
MYL6	P60660	Myosin light polypeptide 6
PRKRIP1	Q9H875	PRKR-interacting protein 1
PSMD8	P48556	26S proteasome non-ATPase regulatory subunit 8
RPS15	P62841	40S ribosomal protein S15
SMG7	Q92540	Protein SMG7
TEKT5	Q96M29	Tektin-5
YBX1	P67809	Nuclease-sensitive element-binding protein 1
Human DNA sequence from clone RP11-543N17 on chromosome 10, complete sequence		

GSK3 phosphorylation site, previously des

Nr of clones	GSK3 phosphorylation site
1	Yes
1	Yes
1	Yes
1	
1	Yes
1	
2	Yes
2	
2	
1	
1	
2	
2	
2	
2	
1	Yes
1	Yes
1	
1	

cribed GSK3 interactor, presence on mammalian testis and sperm and alteration on asthenozoosper

Previously known GSK3 interactor (DOI or PMID)
GSK3α and GSK3β [10.1016/j.celrep.2013.03.027] [10.1038/nmeth.2400] [10.1038/79039] [1
GSK3α and GSK3β [10.1038/nmeth.2400] [10.1016/j.cell.2012.06.047] [10.1038/onc.2012.31
GSK3α and GSK3β [10.1038/nmeth.2400] [10.1016/j.cell.2012.06.047] [10.1038/onc.2012.31
GSK3β [10.1016/j.febslet.2005.08.075]

:issue expression (HPA RNA expression) of testis GSK3β interactors. Mixed expression is defined as l

Present in testis and/or sperm (DOI or PMID)
Human testis and human sperm [10.1006/dbio.2000.9725]
Human testis [10.1038/sj.onc.1204098]
Human testis and sperm (elongating spermatids, pachytene spermatocytes, posterior head of mature
Mouse testis and human sperm [10.1371/journal.pgen.1004825] [10.1371/journal.pone.0127007]
Mouse testis (mRNA) and human sperm [10.1177/1933719112452939] [10.1371/journal.pone.0115ε
Rat testis (Sertoli cells) and human sperm [10.1095/biolreprod.107.062679] [10.1128/MCB.25.10.425
Mouse testis [10.1007/s10059-013-2271-3]
Mouse sperm (manchete of elongating spermatids) [0.1073/pnas.1424648112]
Boar sperm (acrosome) [10.1016/j.jri.2009.11.002]
Mouse testis (spermatocytes and spermatids) [10.1371/journal.pgen.1005863]
Mouse sperm (flagellum, more intense in midpiece) [10.2164/jandrol.109.009456]

tissue-enriched.

Asthenozoospermic alteration (DOI or PMID)	Tissue expression (HPA)
	Mixed
	Ubiquitous
	Group enriched (breast,cerebral cotex, s
	Ubiquitous
	Ubiquitous
	Testis-enriched
	Ubiquitous
	Ubiquitous
Upregulated [10.1074/mcp.M116.061028]	Ubiquitous
Upregulated [10.1074/mcp.M116.061028]	Ubiquitous
	Testis-enriched
Upregulated [10.1074/mcp.M116.061028]	Ubiquitous
	Ubiquitous
	Ubiquitous
	Ubiquitous
	Ubiquitous
Downregulated [10.1074/mcp.M116.061028]	Testis-enriched
	Ubiquitous

alivary glands,testis)

Supplementary Table V. GSK3 isoforms peptides detected on mass spectrometry. Peptide s

Sequence	Start	End	Coverage	Spectral Count
Mass spectrometry eluted with 50mM glycine and 1% SDS				
GSK3a (UniProtKB: P49840)				
TSSFAEPGGGGGGGGGGPGGSASGPGGTGGGK	19	50	10%	5
VTTVVATLGQGPER	100	113		
GSK3b (UniProtKB: P49841)				
TPPEAIALCSR	309	319	3%	1
Mass spectrometry on-bead trypsin digestion				
GSK3a (UniProtKB: P49840)				
VTTVVATLGQGPER	100	113	8%	13
SQEVAYTDIK	114	123		
DIKPQNLLVDPDTAVLK	244	260		
GSK3b (UniProtKB: P49841)				
VTTVVATPGQGPDRPQEVSYTDTK	37	60	17%	32
DTPALFNFTTQELSSNPPLATILIPPHAR	355	383		
IQAAASTPTNATAASDANTGDR	384	405		

sequence, first and last aminoacid of the peptide, peptide % of coverage for the complete proteir

n and peptide spectral count.

Supplementary Table VI.GSK3α human sperm interactors. Gene name, UniProtKB, n

Gene Name	UniProtKB	Name	Spectral Count ratio*†
ARG1	P05089	Arginase-1	GSK3a only
GGCT	O75223	Gamma-glutamylcyclotransferase	GSK3a only
HIST1H2AD	P20671	Histone H2A type 1-D	3
TLR9	Q9NR96	Toll-like receptor 9	GSK3a only
SBSN	Q6UWP8	Suprabasin	GSK3a only
HIST1H4A	P62805	Histone H4	3
HIST1H2BK	A0A024RCL8	Histone H2B	GSK3a only
HSPA5	P11021	78 kDa glucose-regulated protein	GSK3a only
ACR	P10323	Acrosin	
CPZ	Q66K79	Carboxypeptidase Z	
EEF1G	P26641	Elongation factor 1-gamma	
LTF	P02788	Lactotransferrin	
PRSS37	A4D1T9	Probable inactive serine protease 37	
RPL13	P26373	60S ribosomal protein L13	
RPL6	Q02878	60S ribosomal protein L6	
RPS18	P62269	40S ribosomal protein S18	
RPS8	P62241	40S ribosomal protein S8	

* Spectral counts ratios: total number of spectral counts for each protein in GSK3a condition

±†Logarithm of GSK3a/Negative control:

† Mass spectrometry results present distinct scoring methods, since the technique was perfo

r of clones, GSK3 phosphorylation site, previously described GSK3 interactor, preser

Log of GSK3a/NC ratio±†	GSK3 phosphorylation site	Previously known GSK3 interactor (
	Yes	
	Yes	
	Yes	GSK3β [10.1038/nmeth.2400]
8		GSK3β [10.1038/nmeth.2400]
4.8		
4.3		GSK3β [10.1038/nmeth.2400]
6.7		
4.8		
6.9		
4.8		
8.1		
4.4		

divided by the number of total number of spectral counts for each protein in negative contr

rmed in two different facilities, VIB Proteomics Expertise Center and Proteomic Core Lab, Le ıce on mammalian testis and sperm and alteration on asthenozoosperı

Present in testis and/or sperm (DOI or PMID)
Human sperm (activity) [10.1007/s002400050004]
Human testis (Sertoli and Leydig cells) and epididymis [10.1369/0022155411
Mouse sperm (acrosome), human testis and sperm(mRNA) [https://doi.org/1
Mouse testis (spermatocyte) and human sperm [10.1262/jrd.2014-018]
Human testis (mRNA) and sperm [10.1074/jbc.M206065200]
Yes, human testis and sperm (acrosome) [1821849] [4262344] [https://doi.oı
Human sperm [10.1074/mcp.M110.007187]
Human sperm (acrosome) [10.1093/abbs/gmw096]
Human sperm [10.1021/pr500652y]
Yes, human testis and sperm (acrosome) [1821849] [4262344] [https://doi.oı

ol. Only rations higher than 2 were considered relevant (increase of 100% of r

rner Research Institute

ıic samples and tissue expression (HPA RNA expression) of testis GSK3α interactors. Mixe

Asthenozoospermic alteration (DOI or PMID)
428468]
Upregulated [10.1074/mcp.M116.061028]
l0.1274/jmor.27.136] [10.1111/and.12149] [24639717]
Downregulated and Upregulated [10.1007/s00345-013-1023-5] [10.1074/mcp.M116.061028]
Downregulated [10.1074/mcp.M116.061028]
Downregulated [10.1074/mcp.M116.061028]
Downregulated [10.1074/mcp.M116.061028]
rg/10.1016/S0015-0282(16)60021-3]

ıumber of spectral counts in the condition GSK3a). Please note that “GSK3a only” means that spectr

ed expression is defined as being expressed in at least one tissue but in neither ubiquitou

Tissue expression (HPA)
Tissue enhanced (bone marrow, liver)
Ubiquitous
Tissue enhanced (bone marrow, prostate)
Tissue enhanced (lymph node)
Group enriched (esophagus, skin)
Mixed
Ubiquitous
Ubiquitous
Testis-enriched
Ovary-enriched
Ubiquitous
Tissue enhanced (bone marrow, cervix, uterine)
Testis-enriched
Ubiquitous
Ubiquitous
Ubiquitous
Ubiquitous

al counts were only detected in GSK3a condition.

Supplementary Table VII. GSK3β human sperm interactors. Gene name, UniProtKB, mass spec

Gene Name	UniProtKB	Name
ANXA1	P04083	Annexin A1
ARG1	P05089	Arginase-1
BPIFB1	Q8TDL5	BPI fold-containing family B member 1
CASP14	P31944	Caspase 14
CAT	P04040	Catalase
CTSG	P08311	Cathepsin G
LYZ	B2R4C5	C-type lysozyme
DMBT1	Q9UGM3	Deleted in malignant brain tumors 1 protein
GGCT	O75223	Gamma-glutamylcyclotransferase
GSN	P06396	Gelsolin
GAPDH	P04406	Glyceraldehyde-3-phosphate dehydrogenase
HP	P00738	Haptoglobin
HSP90AB1	P08238	Heat shock protein HSP 90-beta
HSPA2	P54652	Heat shock-related 70 kDa protein 2
HIST1H2AD	P20671	Histone H2A
HIST1H2BK	A0A024RCL8	Histone H2B
H3F3B	P84243	Histone 3.3
HIST1H4A	P62805	Histone H4
HIST1H3A	P68431	Histone H3
MUC5AC	A7Y9J9	Mucin 5AC, oligomeric mucus/gel-formin
MPO	P05164	Myeloperoxidase
PFN1	P07737	Profilin-1
S100A8	P05109	Protein S100-A8
DKFZp686J11235	Q6MZW0	Putative uncharacterized protein DKFZp686J11235
SERPINB4	P48594	Serpin B4 (Fragment)
TLR9	Q9NR96	Toll-like receptor 9
n/a	Q6GMV8	Uncharacterized protein
ZG16B	Q96DA0	Zymogen granule protein 16 homolog B
ACR	P10323	Acrosin
LTF	P02788	Lactotransferrin
PRSS37	A4D1T9	Probable inactive serine protease 37
RPL13	P26373	60S ribosomal protein L13
RPL6	Q02878	60S ribosomal protein L6
RPS18	P62269	40S ribosomal protein S18

* Spectral counts ratios: total number of spectral counts for each protein in GSK3β condition di
±†Logarithm of GSK3β/Negative control:
† Mass spectrometry results present distinct scoring methods, since the technique was perform

:trometry score, GSK3 phosphorylation site, previously described GSK3 interact

Spectral counts ratio*	Log of GSK3b/NC ratio±†	GSK3 phosphorylation site
GSK3b only		
GSK3b only		Yes
GSK3b only		
GSK3b only		
GSK3b only		
GSK3b only		
GSK3b only		
GSK3b only		Yes
GSK3b only		Yes
GSK3b only		
2		
GSK3b only		
GSK3b only		
3		
4		
GSK3b only		
GSK3b only		
13		
GSK3b only		
GSK3b only		
GSK3b only		Yes
GSK3b only		
3		
GSK3b only		Yes
GSK3b only		
GSK3b only		
GSk3b only		
GSK3b only		
	7.7	
	6.45	
	4.4	
	4.79	
	4.75	

vided by the number of total number of spectral counts for each protein in nega

ıed in two different facilities, VIB Proteomics Expertise Center and Proteomic Coı

tor, presence on mammalian testis and sperm, alte

Previously known GSK3 interactor (DOI or PMID)
GSK3β [10.1126/scisignal.2001699]
GSK3β [10.1038/nmeth.2400]
GSK3α and GSK3β [10.1038/nmeth.2400]
GSK3β [10.1038/nmeth.2400]
GSK3β [10.1038/nmeth.2400]

ıtive control. Only rations higher than 2 were considı

re Lab, Lerner Research Institute

eration on asthenozoospermic samples and tissue expression (HPA RNA expression) of sperm GSK3b

Present in testis and/or sperm (DOI or PMID)
Human sperm (activity) [10.1007/s002400050004]
Human sperm (catalase activity) [10.1002/mrd.1120240206]
Human testis (Sertoli and Leydig cells) and epididymis [10.1369/0022155411428468]
Boar sperm (fibrous sheat of the flagellum) [9264469]
Rat testis (mRNA) [9432136]
Rat testis (Sertoli cells) and human sperm [10.1095/biolreprod.107.062679] [10.1128/MCB.25.10.425
Mouse testis (spermatogonia, leptotene spermatocytes, pachytene spermatocytes and elongating spe
Mouse testis (spermatocyte) and human sperm [https://doi.org/10.1262/jrd.2014-018] [10.1002/jcb
Human sperm (nuclear) [10.1186/1471-213X-8-34]
Seminal plasma [10.1111/andr.12327]
Rat testis (Leydig and Sertoli cells) [https://doi.org/10.1002/j.1939-4640.2004.tb03175.x]
Human sperm [10.1002/pmic.200600094]
Mouse sperm (acrosome) and human testis and sperm (mRNA) [https://doi.org/10.1274/jmor.27.136
Yes, human testis and sperm (acrosome) [1821849] [4262344] [https://doi.org/10.1016/S0015-0282(
Human sperm (mRNA) [10.1093/humrep/des074]
Human sperm [10.1074/mcp.M110.007187]

ered relevant (increase of 100% of number of spectral counts in the condition GSK3β). Please note tha

Asthenozoospermic alteration (DOI or PMID)

Upregulated [10.1021/pr500652y]
Upregulated [10.1074/mcp.M116.061028]

Downregulated [10.1074/mcp.M116.061028]
Upregulated [10.1074/mcp.M116.061028]
Downregulated [10.1074/mcp.M116.061028]

Downregulated [10.1074/mcp.M116.061028]

vere only detected in GSK3β condition.

Tissue Expression
Esophagus-enriched
Tissue enhanced (bone marrow, liver)
Tissue enhanced (cervix, uterine, stomach)
Skin-enriched
Ubiquitous
Bone marrow-enriched
Ubiquitous
Tissue enhanced (duodenum, small intestine)
Ubiquitous
Ubiquitous
Ubiquitous
Liver-enriched
Ubiquitous
Testis enhanced
Tissue enhanced (bone marrow, prostate)
Ubiquitous
Ubiquitous
Mixed
Group enriched (bone morow, epididymis, testis)
Stomach-enriched
Bone marrow-enriched
Ubiquitous
Group enriched (bone morow, esophagus, tonsil)
no information
Esophagus-enriched
Tissue enhanced (lymph node)
no information
Salivary gland-enriched
Testis-enriched
Tissue enhanced (bone marrow, cervix, uterine)
Testis-enriched
Ubiquitous
Ubiquitous
Ubiquitous

Supplementary Table VIII. Testis expression levels of GSK3α interactome. Expression

Gene Name	UniProtKB
TTC16	Q8NEE8
DDI1	Q8WTU0
LRRC37A2	A6NM11
GOLGA6C	A6NDK9
DRC1	Q96MC2
BCCIP	Q9P287
HSP90AB1	P08238
RUNX1	Q01196
HSP90AA1	P07900
DCP1B	Q8IZD4
MAEA	Q7L5Y9
SBNO1	A3KN83
NBR1	Q14596
SUGP2	Q8IX01
PSMD8	P48556
MYL12A	P19105
ALKBH3	Q96Q83
HMGN1	P05114
DNAJB1	P25685
DEAF1	O75398
H2AFV	Q71UI9
CCDC174	Q6PII3
AURKAIP1	Q9NWT8
SMG7	Q92540
RPL19	P84098
C11orf98	E9PRG8
AP3D1	O14617
CNTROB	Q8N137
PTMA	P06454
RPS15	P62841
VCPIP1	Q96JH7
LDHA	P00338
SMARCA5	O60264
LRP6	O75581
DCAF8	Q5TAQ9
FBXO42	Q6P3S6
AXIN2	Q9Y2T1
MTCH1	Q9NZJ7
AKAP11	Q9UKA4
RPL29	P47914
UBTF	P17480
CHTOP	Q9Y3Y2
RPS19	P39019

RPL15	P61313
HNRNPM	P52272
HMBS	P08397
RefSeqGene on chromosome 5 Chromosome 5: 150,401,911-150,402,122	
Human Dna sequence from clone RP11-543N17	
Homo Sapiens Chromosome 21 clone CTD-250 3J9 map p11-q21.1	
ARG1	P05089
GGCT	O75223
HIST1H2AD	P20671
TLR9	Q9NR96
SBSN	Q6UWP8
HIST1H4A	P62805
HIST1H2BK	A0A024RCL8
HSPA5	P11021
ACR	P10323
PRSS37	A4D1T9
RPS18	P62269
RPL13	P26373
LTF	P02788
RPL6	Q02878
CPZ	Q66K79
RPS8	P62241
EEF1G	P26641
TUBG1	P23258
RAE1	P78406
FOXM1	Q08050
AXIN1	O15169-2
CTNNB1	B4DGU4
PKM	P14618-1
AXIN1	O15169
YWHAG	P61981
FRAT1	Q92837
GSKIP	Q9P0R6
NBR1	Q14596
MAPT	P10636
PRKACA	P17612
DEAF1	O75398
GSK3A	P49840
AIM1	Q9Y4K1
AKAP9	Q99996
AR	P10275
AXIN2	Q9Y2T1
CTNNA1	P35221
PPP1R2	P41236
MDN1	Q9NU22
PSMD1	Q99460

POLR3B	Q9NW08
ZDHHC17	Q8IUH5
AKT1	P31749
PRKCA	P17252
PRKCB	P05771
PRKCD	Q05655
PRKCG	P05129
APP	P05067
ARHGEF11	O15085
PKM	P14618
KRBA1	A5PL33
LRP6	O75581
MAP3K11	Q16584
MYC	P01106
SPICE1	Q8N0Z3
VTA1	Q9NP79
EIF2B5	Q13144
PRKD3	O94806
SGK3	Q96BR1
CTNNB1	P35222
FCGR2B	P31994
HDAC6	Q9UBN7
HSP90AA1	P07900
HSP90AB1	P08238
PPP3CC	P48454
RCAN2	Q14206
SPG21	Q9NZD8
TRAK2	O60296
BICD1	Q96G01
CREM	Q03060
GSK3B	P49841
HSF1	Q00613
PRKCZ	Q05513
MCL1	Q07820
SGK1	O00141
BCL3	P20749
CREB1	P16220
EBNA1BP2	Q99848
GLI3	P10071
PRKCH	P24723
LRSAM1	Q6UWE0
PXN	P49023
PRKDC	P78527
RICTOR	Q6R327
ARSG	Q96EG1
PPP1CA	P62136

PPP1CB	P62140
PPP1CC	P36873
PPP3CB	P16298
RCAN1	P53805
SAMHD1	Q9Y3Z3
SRBD1	Q8N5C6

levels of all GSK3 interactors were retrieved form the human protein atlas, PaGeneBase, E

HPA protein expression	HPA mRNA expression values	BioGPS	PaGenBAse	Expression Atlas
Group enriched	58.280	n/a	97.390	62.500
Testis enriched	100	8.1872	99.980	100.000
Testis enriched	77.632	6.9583		4.501
Testis enriched	n/a	n/a	99.130	100.000
Group enriched	33.981	6.7664		42.182
		7.465		1.989
		2.813		0.638
		4.153		1.989
		7.716		6.215
		9.249		6.215
		3.224		2.942
		6.099	90.270	3.279
		6.828		4.008
		10.4925	94.970	8.165
		7.0089		4.278
		4.2957		0.894
		5.2179		3.084
		3.0988		2.702
		13.3536		6.369
		2.7794		2.212
		3.5285		1.729
		5.3921		3.024
		11.6677		7.807
		7.2974	100.000	5.770
		3.8772		1.342
		5.8485		3.237
		4.0967		4.061
		n/a		10.087
		1.9029		2.292
		3.1992		2.331
		4.8426		3.950
		2.9166		1.275
		4.4525		4.536
		5.1604		2.004
		3.7098		2.476
		4.9336		2.722
		5.2514		2.618
		2.1634		1.506
		2.6625		3.315
		3.3782		1.518
		3.5255		1.845
		3.4345		2.404
		2.9667		1.669

		4.0430		1.884
		3.2171		1.632
		0.5810		1.548
		1.5534		0.372
		2.6738		1.359
		4.4163		5.946
		n/a		n/a
		n/A		0.018
		4.2962		0.000
		3.0936		4.816
		5.2981		2.576
Testis enriched	88.003	13.1225	99.243	97.074
Testis enriched	98.039	n/a	95.190	100.000
		4.0987		1.034
		4.0238		1.730
		0.2265		0.000
		1.9018		0.875
		4.5534		1.011
		1.9940		0.801
		4.5537		0.801
Testis enriched	22.926	33.6003	96.310	47.926
Testis enriched	22.507	33.1143	92.760	37.495
Testis enriched		8.1761	100.000	10.832
		4.0168		2.963
		3.3887		1.586
		2.8176		70.164
		4.0168		2.963
		n/a		1.277
		1.1796		8.910
		7.7826		2.839
		6.8276		4.008
		1.3419		0.426
		6.2514		9.405
		2.7794		3.318
		5.8364		3.139
		0.6990		1.106
		1.7124		1.356
		4.4957		1.376
		5.2514		2.618
		2.2363		1.191
		13.6660		4.351
		5.4885		4.111
		3.4812		2.533

5.5611		77.500
1.6730		2.241
2.0556		1.754
1.6213		0.357
0.4333		1.599
1.3960		1.970
4.9301		1.055
2.6173		1.707
5.2436		4.937
2.8176		1.809
n/a		3.116
5.1604		2.004
3.3841		1.820
1.6741		0.896
5.2394		3.075
4.1524		1.801
3.2238		1.834
4.4915		4.739
3.6034		2.622
3.3887		1.586
1.6268		0.000
6.2662		4.036
7.7165		6.215
2.8133		0.638
9.1377		7.567
0.8041		0.722
3.4387		2.117
0.8052		1.024
4.5969		0.958
18.4107	100.000	13.194
9.7621		3.821
8.9501	100.000	10.395
6.5738		6.712
2.1370		1.019
2.2366		1.617
2.5430		1.364
8.8291		31.770
4.7800		5.125
5.8729		1.051
1.0615		1.245
5.1593		1.042
3.4225		1.606
1.9427		5.699
0.7627		1.906
0.9868		1.777
0.5964		1.321

0.4761	1.355
1.0016	2.781
0.7151	1.223
0.2592	0.886
1.1670	1.139
69.8440	3.390

Expression atlas, BioGPS and UniGene testis ex

Unigene	
54.5455	
94.6809	
6.4039	All values wer
76.4706	n/a
35.6322	50% of expres
1.8802	
2.3966	
0.5076	
2.4068	
9.9469	
2.6919	
4.7818	
9.0416	
17.3305	
2.1676	
0.4758	
4.7364	
1.9984	
6.1558	
2.1662	
n/a	
1.8692	
1.9175	
4.3344	
0.5235	
1.1065	
2.4658	
2.3272	
0.7693	
0.8969	
3.4043	
1.3008	
4.4765	
1.5734	
3.1735	
5.0871	
5.2439	
2.1710	
0.9194	
0.4976	
1.4398	
3.4414	
0.7131	

1.5560
0.8464
0.9382
0.0000
0.3583
16.6667
0.0000
0.0000
0.0000
0.8604
1.9065
56.5217
20.6107
0.3479
0.6172
0.0442
1.1071
1.4129
0.5373
0.9917
5.6788
9.4287
1.8096
1.5810
2.0449
1.8676
1.5810
0.8662
2.4658
1.8685
9.0416
1.4540
1.8443
2.1662
0.6224
1.4870
1.1595
4.4776
5.2439
2.3746
6.8942
2.0619
3.0429

3.8570
1.5069
0.4581
0.0000
1.5704
2.7434
4.6243
3.1995
2.6675
1.8676
2.0067
22.8298
3.8974
0.2859
1.5134
1.4496
1.2312
2.8740
2.3013
2.0449
0.0000
6.0943
2.4068
2.3966
8.3790
4.4461
1.3519
1.2016
2.5400
13.3431
2.3665
3.3739
4.4717
2.0599
1.0382
0.1428
3.8528
1.9390
3.6165
1.7349
1.2432
3.9199
1.1814
0.6587
1.5326
0.6517

1.5075
3.3235
3.7766
0.9187
0.9662
6.7864

xpression values were normalized. Yellow: GSK3α testis interactors; Green: GSK3α sp

Testis YTH identified interactors
Sperm Mass Spectometry identified interactors
Databases retrieved interactors
re normalized and presented in % of testis expression compared to the total tissues tested
no information available
ssion in testis in at least 2 databases. Interactors were classified in three categories: 50-75%; 7

›erm interactors; Orange: (

’5%-90 and >90%.

Supplementary Table IX: Testis expression levels of GSK3β interactome. Expression levels (

Gene Name
YBX1
C10orf90
TEKT5
MYL6
DCP1B
BCCIP
HSP90AA1
RPS15
PSMD8
CASC4
CMTM2
LYAR
AXIN2
PRKRIP1
HNRNPM
C11orf98
SMG7
HSP90AB1
Human DNA sequence from clone RP11-543N17 on chromosome 10, complete sequence
HSPA2
ANXA1
ARG1
BPIFB1
CASP14
CAT
CTSG
LYZ
DMBT1
GGCT
GSN
GAPDH
HP
HSP90AB1
HIST1H2AD
HIST1H2BK
H3F3B
HIST1H3A
HIST1H4A
MUC5AC
MPO
PFN1
S100A8
DKFZp686J11235

SERPINB4
TLR9
n/a
ZG16B
LTF
ACR
PRSS37
RPL6
RPS18
LTF
RPL13
TUBB1
PFKFB4
AURKA
IQCG
TUBG1
TOP2A
DDX20
IGF2BP1
PBK
SP7
RGS22
HIST1H1T
CABYR
TSKS
PRKACG
FOXM1
AXIN1
MAPT isoform Tau-F
EGLN3
CABYR isoform 5
CABYR isoform 3
MAPT isoform Tau-E
DAB2IP isoform 2
CTNNB1
APC
GSK3B
AKAP11
AKT1
TP53
GSKIP
PRKACA
LRP6
MYC
MAPT
AR

FRAT1
PPP1R2
MUC1
NOTCH1
SGK3
SMAD3
SNAI1
DNM1L
NIN
ACLY
PPP1CA
PTPN1
STRAP
TSC2
ATXN3
PSEN1
AXIN2
PTK2
FRAT2
APP
GYS1
PRKAR1A
PPP1CC
VIM
CCNE1
SMAD1
BTRC
BICD1
EPM2A
NOTCH2
AKT2
HSPA1A
HSPA1B
LRRK2
RELB
UBR5
DEAF1
DHX36
EWSR1
ZFPM1
GEMIN4
SNRNP70
SF3B1
SMN1
SMYD2
XPO6

HSP90AA1
KLF5
MAP3K1
SNAI2
CDH1
FZR1
ANKRD6
CLASP2
DAB2IP
DYNLL1
E2F1
EPB41L3
PRKAR2A
PRUNE1
RPF2
RELA
TRAF2
TANK
TSC1
MAPK1
NBR1
BCL3
CCND1
HSPA4
NFKB1
SNCAIP
ARHGEF11
KRBA1
SFPQ
SPICE1
VTA1
EIF2B5
JUN
PRKCB
CREB1
DACT1
DDIT4
EYA1
FOXO1
PRKCA
PRKCZ
MDM2
IKBKG
NFE2L1
NFE2L3
PHLPP1

PPARGC1A
TAZ
WWTR1
YWHAZ
PPP2R5D
EIF4EBP1
ACACA
ACSBG1
DBI
ACTL6B
ACTBL2
ADAP1
ADIRF
PMAIP1
ASRGL1
ATF3
ATPIF1
BAG6
BEX1
BHLHE41
BIRC2
BIRC3
BRIX1
BZW2
CAMSAP3
CCDC6
CDC37
CEBPB
CEBPZ
CENPB
CHD3
CRELD2
CSAD
CSF3R
CSNK2B
COPS5
GJB5
CSTB
CST6
DCD
DCTN3
DDX5
BHLHE40
DEC1
DEFA1
HSD17B4

DHX34
DNAJC13
DNMT3L
DNMT1
DUSP9
EEF1A1
EEF1G
ELAVL1
IKBKAP
MPP1
ENTPD6
C14orf1
FAM83D
FBN3
FBXW11
FBXW7
FEN1
IFT46
VPS51
FIBP
FIP1L1
FKBP14
KHSRP
FUS
FZD5
GAPDH
GNB2
GBP2
GIPC1
GPR39
HSPA9
HSPA5
HIST1H1C
HIST1H1E
H1FX
HAX1
HBA1
HDAC6
HECW2
HRNR
HP
HSP90AB1
HSPA8
CLNS1A
IGHM
IGSF21

ILK
ITLN1
KANK1
KIF5B
LUC7L2
LMO4
MID1IP1
MAP3K11
MAP1A
MAP4
MASP1
MCCC2
MED24
MICAL1
MKL1
MAP2K5
MTF2
MTOR
MYCN
MYH9
NAT9
MGEA5
NOTCH3
NRBP1
IVNS1ABP
NSFL1C
NUB1
NUFIP1
KIAA1191
PIM2
PPP3CC
PRDX1
PTBP3
PTN
QPCTL
RAI1
RASSF1
RCAN2
UPF3A
RPL13
RPL19
RPL23
RPL23A
RPL27A
RPL29
RPL31

RPL35
RPL36A
RPL36AL
RPL37
RPL37A
RPL8
RPLP1
RNF220
POLR2B
RPS11
RPS14
RPS16
RPS17
RPS18
RPS19
RPS23
RPS24
RPS25
RPS27A
RPS29
RPS2
FAU
RPS4X
RPS6
RSU1
RXRA
SAP30BP
SF3A1
SHROOM3
SLA
SMARCA2
SMARCA5
SMURF2
SPTBN4
STK11
RBPJ
SYNE4
EPRS
QARS
TUBA1A
TUBB
TBC1D4
CLEC3B
TLE1
TMEM44
TONSL

TRAK2
TRAP1
HSP90B2P
TRIM29
PRSS3
EFTUD2
UBE2D1
UBR1
UBXN6
UFM1
WSB1
XIAP
ERCC4
XPO1
XPNPEP1
YAP1
ZHX1
ZKSCAN2
ZNF135
ZNF227
ZNF746
HNRNPD
YBX3
YBX1
SNCA
CREM
DPYSL2
GSK3A
MCL1
MYOCD
OGT
PCM1
MBD1
SGK1
TPPP
AKT3
ARRB1
BICD2
CIITA
CDK5
CDX2
CEBPA
CREB3L3
CTNND1
DYNC1I1
DCTN1

DCTN2
HDAC4
KLF2
RPS6KA1
MAP3K4
MAP1B
MARK2
MITF
NCOA3
NFE2L2
PIK3R1
PXN
PDE4D
PRKDC
RCAN1
RICTOR
SREBF1
TMEM132A
FZD1
GRB14
ILKAP
MAP2K7
PPP2CA
PTPN11
AMMECR1
STYK1
YWHAQ
APC2
APOC2
SLC25A23
ANAPC2
CDKN1B
CREB3
DVL2
DVL3
GLI2
GYS2
PIN1
PRKX
CD274
PIAS1
DEFA5
DKK3
KIAA0317
MAP3K2
NFATC1

NFATC2
PPP1CB
SAMHD1
TBK1
U2AF1
UBE3A
UBXN2B
SOX10
LPCAT1
SOX9

of all GSK3 interactors were retrieved form the human protein atlas, PaGeneBase, Expressior

UniProtKB	HPA protein expression	HPA mRNA expression values	BioGPS	PaGenBAse
P67809	Testis enriched	10.069	19.344	
Q96M02	Group enriched	29.524	5.686	
Q96M29	Testis enriched	90.982	5.810	99.940
P60660			3.752	
Q8IZD4			9.249	
Q9P287			7.465	
P07900			7.716	
P62841			3.199	
P48556			7.009	
Q6P4E1			5.355	
Q8TAZ6			91.946	99.050
Q9NX58			8.383	
Q9Y2T1			5.251	
Q9H875			4.487	
P52272			3.217	
E9PRG8			5.849	
Q92540			7.297	100.000
P08238			2.813	
P54652	Testis enhanced	21.975	25.788	
P04083			0.328	
P05089			1.553	
Q8TDL5			0.101	
P31944				
P04040			0.304	
P08311			1.405	
B2R4C5			0.053	
Q9UGM3			0.616	
O75223			2.674	
P06396			3.658	
P04406			2.819	
P00738			0.241	
P08238			2.813	
P20671			4.416	
A0A024RCL8			3.094	
P84243			6.526	
P68431			3.865	
P62805			4.296	
A7Y9J9			2.936	
P05164			0.188	
P07737			1.098	
P05109			0.040	
Q6MZW0				

P48594			4.316	
Q9NR96				
Q6GMV8				
Q96DA0			0.205	
P02788			0.226	
P10323	Testis enriched	88.003	13.123	99.243
A4D1T9	Testis enriched	98.039	n/a	99.243
Q02878			1.902	
P62269			4.099	
P02788			0.226	
P26373			4.024	
Q9H4B7	Group enriched	7.772	4.396	
Q16877	Testis enhanced	15.403	4.979	
O14965	Testis enhanced	21.176	5.346	100.000
Q9H095	Group enriched	21.801	27.314	
P23258	Testis enriched	22.926	33.600	96.310
P11388	Testis enhanced	23.397	5.582	98.940
Q9UHI6	Testis enriched	34.621	21.891	96.290
Q9NZI8	Group enriched	46.392	5.675	99.760
Q96KB5	Testis enriched	49.521	35.900	99.620
Q8TDD2	Testis enhanced	52.000	5.707	
Q8NE09	Testis enriched	67.038	18.230	94.990
P22492	Testis enriched	82.353	4.893	100.000
O75952	Testis enriched	83.106	84.722	100.000
Q9UJT2	Testis enriched	89.728	69.429	99.400
P22612	Testis enriched	100.000	8.082	100.000
Q08050	Testis enhanced	17.914	8.176	100.000
O15169			4.017	
P10636-8				
Q9H6Z9			4.615	
O75952-5				
O75952-3				
P10636-7				
Q5VWQ8-2				
P35222			3.389	
P25054			2.634	
P49841			9.762	
Q9UKA4			2.662	
P31749			2.056	
P04637			2.093	
Q9P0R6			7.783	
P17612			6.251	
O75581			5.160	
P01106			1.674	
P10636			1.342	
P10275			4.496	

Q92837	1.180	
P41236	13.666	
P15941	2.606	
P46531	3.232	
Q96BR1	3.603	
P84022	2.954	
O95863	4.945	
O00429	3.544	
Q8N4C6	4.587	
P53396	1.748	
P62136	1.388	
P18031	3.272	
Q9Y3F4	3.863	
P49815	5.839	
P54252	4.578	
P49768	5.176	
Q9Y2T1	5.251	
Q05397	5.014	
O75474	0.799	
P05067	2.617	
P13807	1.417	
P10644	3.654	
P36873	9.123	
P08670	3.105	
P24864	2.436	
Q15797	5.823	
Q9Y297	5.068	99.790
Q96G01	4.597	
B3EWF7	4.544	99.000
Q04721	7.617	
P31751	4.826	
P0DMV8	2.114	
P0DMV9	2.104	
Q5S007	4.442	
Q01201	2.857	
O95071	14.209	
O75398	2.779	
Q9H2U1	5.258	
Q01844	6.700	
Q8IX07	5.725	100.000
P57678	35.724	
P08621	3.412	
O75533	3.605	
Q16637	5.355	
Q9NRG4	9.587	
Q96QU8	5.139	

P07900	7.716	
Q13887	2.608	
Q13233	4.621	
O43623	0.973	
P12830	0.331	
Q9UM11	6.686	100.000
Q9Y2G4	4.378	
O75122	0.813	
Q5VWQ8	3.848	
P63167	8.488	
Q01094	4.478	
Q9Y2J2	3.368	
P13861	7.101	99.200
Q86TP1	4.064	
Q9H7B2	5.364	
Q04206	3.570	
Q12933	4.580	
Q92844	3.249	
Q92574	4.056	
P28482	2.857	
Q14596	6.828	
P20749	2.543	
P24385	0.613	
P34932	6.069	
P19838	1.102	
Q9Y6H5	4.759	
O15085	5.244	
A5PL33	n/a	
P23246	3.975	
Q8N0Z3	5.239	
Q9NP79	4.152	
Q13144	3.224	
P05412	2.210	
P05771	0.433	
P16220	8.829	
Q9NYF0	2.416	
Q9NX09	0.625	
Q99502	3.458	
Q12778	4.173	
P17252	1.621	
Q05513	6.574	
Q00987	4.676	
Q9Y6K9	3.245	
Q14494	4.183	
Q9Y4A8	2.715	
O60346	2.016	

Q9UBK2	4.077	
Q16635	4.449	
Q9GZV5	2.574	
P63104	3.277	
Q14738	5.583	
Q13541	2.082	
Q13085	4.044	
Q96GR2	2.867	
P07108	5.130	
O94805	2.644	
Q562R1	5.664	
O75689	2.714	
Q15847	1.455	
Q13794	0.565	
Q7L266	58.457	95.510
P18847	1.832	
Q9UII2	8.739	
P46379	17.144	
Q9HBH7	3.275	
Q9C0J9	0.644	
Q13490	3.321	
Q13489	1.109	
Q8TDN6	4.631	
Q9Y6E2	1.855	
Q9P1Y5	5.633	
Q16204	4.519	
Q16543	2.577	
P17676	0.620	
Q03701	7.483	
P07199	4.280	
Q12873	3.290	
Q6UXH1	6.428	
Q9Y600	3.559	
Q99062	0.365	
P67870	14.192	
Q92905	7.232	
O95377	4.401	
P04080	1.903	
Q15828	2.907	
P81605	0.602	
O75935	1.961	
P17844	4.325	
O14503	0.936	
Q9P2X7	4.927	
P59665	0.074	
P51659	1.411	

Q14147	6.216	
O75165	4.549	
Q9UJW3	4.913	
P26358	3.734	
Q99956	2.464	
P68104	4.440	
P26641	4.554	
Q15717	4.892	
O95163	n/a	
Q00013	1.314	
O75354	3.796	
Q9UKR5	4.979	100.000
Q9H4H8	1.490	
Q75N90	5.543	
Q9UKB1	4.321	
Q969H0	1.393	
P39748	1.389	
Q9NQC8	6.212	
Q9UID3	1.850	
O43427	7.377	
Q6UN15	5.734	
Q9NWM8	3.908	
Q92945	6.472	
P35637	5.013	
Q13467	2.929	
P04406	2.819	
P62879	3.486	
P32456	2.010	
O14908	3.942	
O43194	3.955	
P38646	2.771	
P11021	5.298	
P16403	1.193	
P10412	4.780	
Q92522	1.090	
O00165	6.033	
P69905	5.211	
Q9UBN7	6.266	
Q9P2P5	5.688	
Q86YZ3	5.668	
P00738	0.241	
P08238	2.813	
P11142	2.905	
P54105	1.619	
P01871	0.579	
Q96ID5	0.832	

Q13418	3.423	
Q8WWA0	4.836	
Q14678	3.054	
P33176	9.060	
Q9Y383	3.928	
P61968	1.541	
Q9NPA3	2.715	
Q16584	3.384	
P78559	0.962	
P27816	3.060	
P48740	4.979	
Q9HCC0	3.127	
O75448	4.043	
Q8TDZ2	2.106	
Q969V6	4.822	
Q13163	4.916	
Q9Y483	5.122	
P42345	6.328	100.000
P04198	4.474	
P35579	1.839	
Q9BTE0	4.419	
O60502	2.529	
Q9UM47	3.756	
Q9UHY1	6.579	
Q9Y6Y0	2.885	
Q9UNZ2	3.765	
Q9Y5A7	5.622	
Q9UHK0	4.686	100.000
Q96A73	1.056	
Q9P1W9	2.836	
P48454	9.138	
Q06830	1.790	
O95758	4.439	
P21246	4.140	
Q9NXS2	4.809	
Q7Z5J4	4.847	
Q9NS23	1.216	
Q14206	0.804	
Q9H1J1	10.448	
P26373	4.024	
P84098	3.877	
P62829	2.651	
P62750	4.062	
P46776	2.706	
P47914	3.378	
P62899	4.163	

P42766	3.285	
P83881	1.656	
Q969Q0	2.755	
P61927	3.393	
P61513	6.239	
P62917	2.167	
P05386	3.007	
Q5VTB9	3.978	
P30876	3.979	
P62280	4.564	
P62263	3.387	100.000
P62249	2.831	
P08708	2.864	
P62269	4.099	
P39019	2.967	
P62266	3.349	
P62847	3.360	
P62851	3.320	
P62979	3.500	
P62273	4.707	
P15880	2.518	
P35544	3.214	
P62701	2.634	
P62753	4.570	
Q15404	2.768	
P19793	1.586	
Q9UHR5	2.823	
Q15459	7.101	
Q8TF72	n/a	
Q13239	0.929	
P51531	7.183	
O60264	4.452	
Q9HAU4	5.061	
Q9H254	3.828	
Q15831	3.907	
Q06330	6.047	
Q8N205	5.728	
P07814	2.434	
P47897	2.718	
Q71U36	1.063	
P07437	2.518	
O60343	2.936	
P05452	7.676	
Q04724	5.653	
Q2T9K0	5.573	
Q96HA7	4.906	

O60296	0.805	
Q12931	4.509	
Q58FF3	n/a	
Q14134	1.574	
P35030	0.130	
Q15029	5.751	
P51668	3.664	
Q8IWV7	5.447	
Q9BZV1	7.823	
P61960	2.910	
Q9Y6I7	2.676	
P98170	4.737	
Q92889	5.280	100.000
O14980	4.321	
Q9NQW7	4.185	100.000
P46937	4.339	
Q9UKY1	4.068	
Q63HK3	5.676	
P52742	4.748	
Q86WZ6	4.697	100.000
Q6NUN9	n/a	
Q14103	2.527	
P16989	20.175	
P67809	19.344	
P37840	0.775	
Q03060	18.411	100.000
Q16555	0.305	
P49840	5.836	
Q07820	2.137	
Q8IZQ8	5.678	
O15294	1.207	
Q15154	21.706	
Q9UIS9	5.084	
O00141	2.237	
O94811	1.200	
Q9Y243	2.588	
P49407	2.563	
Q8TD16	2.170	
P33076	4.938	
Q00535	3.838	
Q99626	4.954	
P49715	1.229	
Q68CJ9	4.283	
O60716	5.780	
O14576	0.968	
Q14203	4.442	

Q13561	4.752	
P56524	3.483	
Q9Y5W3	1.413	
Q15418	2.157	
Q9Y6R4	3.714	100.000
P46821	0.729	
Q7KZI7	4.757	
O75030	2.523	
Q9Y6Q9	2.886	
Q16236	4.934	
P27986	1.115	
P49023	3.422	
Q08499	3.364	
P78527	1.943	
P53805	2.791	
Q6R327	5.425	
P36956	4.388	
Q24JP5	1.780	
Q9UP38	2.861	
Q14449	10.469	
Q9H0C8	2.308	
O14733	4.908	
P67775	2.166	
Q06124	2.381	
Q9Y4X0	1.287	
Q6J9G0	4.669	
P27348	5.277	
O95996	3.249	
P02655	1.967	
Q9BV35	4.550	
Q9UJX6	n/a	
P46527	1.814	
O43889	6.065	
O14641	5.552	
Q92997	3.667	
P10070	5.422	
P54840	4.313	
Q13526	5.277	
P51817	2.364	
Q9NZQ7	0.686	
O75925	1.000	
Q01523	0.100	
Q9UBP4	0.700	
O15033	2.405	
Q9Y2U5	0.118	
O95644	0.690	

Q13469	0.100
P62140	0.476
Q9Y3Z3	0.208
Q9UHD2	1.186
Q01081	0.704
Q05086	0.752
Q14CS0	0.708
P56693	0.114
Q8NF37	0.232
P48436	1.528

n atlas, BioGPS and UniGene were retrieved and testis ex

Expression Atlas	Unigene
9.768	1.213
21.151	9.143
100.000	74.627
1.087	0.558
6.215	9.947
3.279	1.880
3.831	2.407
2.331	0.897
4.278	2.168
1.951	1.231
95.434	65.517
48.011	9.365
3.313	0.000
3.680	1.251
3.145	0.846
3.237	1.107
5.770	4.334
10.335	2.397
44.756	15.831
0.106	0.135
0.372	0.000
4.800	0.164
0.000	0.000
0.584	0.946
1.402	0.440
0.057	0.000
0.522	0.073
1.359	0.358
1.069	0.775
33.284	0.914
0.062	4.468
1.989	0.090
5.946	16.667
4.816	0.860
3.023	1.478
n/a	0.000
0.000	0.000
0.000	0.000
0.000	0.064
1.642	0.495
0.072	0.167
n/a	0.154

All values wer

n/a

50% of expres

	0.000	0.135
n/a		0.000
n/a		n7a
	0.024	0.000
	0.000	0.044
	97.074	56.522
	100.000	20.611
	0.875	1.107
	1.034	0.348
	0.000	0.044
	1.730	0.617
	7.816	2.721
	16.322	11.277
	21.512	6.491
	14.232	6.737
	47.926	5.679
	21.396	3.892
	28.066	16.397
	55.000	9.295
	48.805	18.671
	100.000	0.844
	68.887	60.400
	100.000	100.000
	65.792	60.983
	95.210	60.563
	99.187	81.967
	10.832	1.810
	2.963	1.581
n/a		
	0.210	0.845
n/a		
n/a		
n/a		
n/a		
	1.586	2.045
	1.456	3.853
	3.821	2.367
	3.315	0.919
	1.754	0.458
	2.176	1.296
	2.839	1.868
	9.405	1.844
	2.004	1.573
	0.896	0.286
	1.068	1.454
	1.376	4.478

8.910	2.466
4.351	6.894
3.616	0.180
0.980	0.281
2.622	2.301
0.704	0.673
2.427	1.500
2.855	5.705
0.742	1.078
2.648	3.603
1.235	0.652
2.624	3.634
2.455	5.362
4.390	2.689
2.585	2.058
2.864	3.783
3.937	0.000
2.536	2.999
3.540	0.830
1.707	3.199
0.707	1.609
1.946	2.667
3.306	3.324
0.914	0.793
9.355	4.691
3.599	3.574
6.153	3.213
1.438	2.540
2.537	6.888
31.308	3.278
3.246	1.678
1.559	0.435
1.449	0.435
0.586	0.246
1.026	1.453
10.031	1.891
3.318	2.166
4.241	3.359
3.733	1.934
7.206	5.172
13.305	16.493
2.113	1.155
2.552	0.484
3.844	1.006
3.247	1.437
9.910	2.106

3.831	2.407
20.580	2.672
3.124	1.682
0.955	0.000
2.510	0.217
5.163	2.554
2.767	9.430
1.898	1.864
2.379	1.393
4.132	0.691
7.945	1.907
8.300	6.552
5.658	7.746
3.733	3.316
3.091	3.101
1.827	1.526
2.330	3.582
1.573	5.071
4.031	3.598
2.305	2.266
4.008	9.042
1.364	0.143
0.261	0.604
4.339	2.073
1.376	1.875
4.097	6.584
4.937	2.668
3.116	2.007
2.623	1.094
3.075	1.513
1.801	1.450
1.834	1.231
1.003	0.504
1.599	1.570
31.770	3.853
5.692	6.355
0.736	0.632
3.351	2.008
1.567	1.819
0.734	0.000
6.712	4.472
1.894	1.881
3.128	0.111
1.671	2.697
1.201	0.688
4.393	2.492

	26.789	2.281
	0.898	0.429
	0.826	1.159
	1.732	2.760
	3.933	2.643
	0.676	0.987
	4.088	1.531
	145.000	5.744
	3.677	1.119
	1.516	2.326
n/a		0.000
	0.290	0.480
n/a		1.731
	1.231	1.964
	15.964	7.424
	0.475	0.609
	5.890	0.757
	9.143	6.444
	4.943	3.161
	0.909	0.406
	2.609	2.140
	2.609	0.000
	2.845	1.255
	0.887	0.722
	4.457	6.809
	1.684	1.026
	2.426	1.410
	0.334	0.990
	3.599	7.971
	0.949	0.128
	2.249	0.740
	4.943	4.116
	2.836	1.379
	0.000	0.219
	5.648	3.657
	3.432	2.513
	0.978	0.000
	0.593	0.446
	0.566	2.244
	0.000	0.000
	1.810	1.263
	1.727	2.122
	0.572	0.567
	0.572	0.000
	0.000	0.072
	1.049	1.517

	10.194	6.122
	1.965	2.198
	0.000	3.226
	5.025	3.102
	2.914	0.000
	1.714	0.813
	31.776	0.992
	4.686	3.593
	2.114	2.451
	2.984	1.104
	3.048	2.137
	12.792	3.431
	2.366	1.776
	0.000	0.000
	1.888	3.571
	3.239	1.541
	4.952	1.394
	4.714	3.862
	2.108	1.728
	4.512	3.052
	5.634	3.491
	1.438	1.048
	4.592	2.426
	3.561	1.721
	0.332	0.798
	33.284	0.914
	2.121	0.420
	2.605	0.258
	1.334	0.729
	11.964	10.092
	1.896	1.845
	2.576	1.907
	2.313	1.263
	2.911	0.000
	1.408	0.269
	3.271	2.072
	0.065	0.052
	4.036	6.094
	3.781	5.000
n/a		18.182
	0.093	0.090
	10.335	2.397
	3.674	1.756
	2.079	0.807
	0.126	0.162
	0.364	2.326

1.616	1.008
0.382	0.235
2.620	1.584
2.874	1.488
2.621	3.793
1.732	1.024
2.064	1.100
1.820	3.897
2.351	0.406
2.763	1.407
0.000	1.461
1.341	0.665
3.394	8.950
2.241	2.813
3.894	4.331
3.824	4.326
6.975	2.694
7.161	2.948
7.750	0.000
1.007	0.270
2.811	1.233
2.125	1.381
0.830	0.588
3.774	2.258
1.637	2.196
2.176	2.380
3.217	2.122
4.259	6.299
4.259	1.419
1.503	3.278
7.567	8.379
1.205	1.936
3.426	1.754
2.731	0.487
2.162	0.000
2.182	0.000
3.480	1.467
0.722	4.446
5.177	5.974
7.123	0.617
1.342	0.523
1.004	0.580
24.620	0.506
1.018	0.590
1.518	0.498
1.235	0.901

1.765	0.495
1.366	1.280
1.788	1.063
1.409	0.264
22.033	0.427
1.308	0.403
1.027	0.335
5.164	4.186
2.954	4.286
1.150	0.734
1.306	0.345
1.083	0.279
0.921	0.227
1.040	0.348
1.669	0.713
0.962	1.133
1.086	0.537
1.394	0.517
1.020	1.271
1.623	0.759
0.933	0.351
1.520	0.581
0.712	1.080
1.238	0.631
0.976	0.891
1.231	0.478
2.401	1.086
4.758	3.772
0.418	0.739
1.915	0.739
3.670	1.636
4.536	4.476
6.838	1.375
3.856	0.952
40.645	3.115
1.775	2.078
0.606	2.078
2.481	1.563
1.854	1.904
1.196	1.924
9.645	1.582
1.174	1.684
4.513	3.767
3.400	1.612
1.518	1.373
4.575	1.916

1.024	1.202
2.068	2.929
1.212	0.000
0.280	0.433
0.124	0.257
3.856	3.328
1.252	1.144
2.806	2.387
19.471	0.571
1.271	2.149
1.707	2.531
1.204	0.311
6.243	12.060
4.404	3.081
2.056	1.836
1.323	0.320
1.515	1.487
10.231	4.124
4.572	4.083
3.274	3.602
6.086	11.170
2.823	0.853
7.483	4.208
9.768	1.213
0.260	0.645
13.194	13.343
0.905	4.220
3.139	0.622
1.019	2.060
1.376	2.429
0.961	0.786
6.572	4.713
5.699	11.124
1.617	1.038
0.307	0.932
0.535	2.278
0.535	0.372
2.215	0.553
0.451	0.467
1.315	1.299
0.000	0.000
0.000	0.000
0.279	0.000
2.061	2.359
0.685	0.650
3.646	9.848

2.286	2.012
4.037	9.103
1.745	0.000
0.866	1.239
4.329	1.984
1.613	0.899
1.666	0.892
0.493	0.417
1.384	1.560
3.728	1.398
0.788	0.390
1.606	3.920
0.643	3.920
5.699	1.181
0.924	0.919
2.955	0.659
4.546	3.437
1.059	0.143
1.049	1.693
9.840	6.250
2.707	1.347
3.498	7.545
1.948	2.513
0.970	1.057
0.891	2.324
0.000	0.000
2.835	3.247
1.770	0.404
0.000	0.000
0.604	1.050
5.461	3.553
2.211	1.487
3.345	4.973
3.800	5.148
2.099	1.908
5.260	4.962
0.000	0.000
5.338	8.111
5.174	1.643
0.981	1.293
3.401	4.208
0.000	0.000
1.285	2.294
3.883	2.502
2.343	1.888
2.530	2.596

1.429	0.627
1.355	1.508
1.139	0.966
5.418	5.071
2.196	3.192
1.896	2.032
1.667	2.371
0.123	0.718
1.026	0.640
4.476	6.588

xpression values were normalized. Yellow: GSK3β testis interactors; Green: GSK3β sperm int

Testis YTH identified interactors
Sperm Mass Spectometry identified interactors
Databases retrieved interactors
e normalized and presented in % of testis expression compared to the total tissues tested
no information available
ssion in testis in at least 2 databases. Interactors were classified in three categories: 50-75%; 7

teractors; Orange: GSK3β database interactors.

'5%-90 and >90%.

Supplementary Table X. Testis enriched GSK3 interactors. To be classified as

GSK3α interactors		
Gene Name	UniProtKB	Expression
DDI1	Q8WTU0	>90%
GOLGA6C	A6NDK9	>90%
TTC16	Q8NEE8	50% - 75%
ACR	P10323	>90%
PRSS37	A4D1T9	>90%

50% of expres

GSK3β interactors		
Gene Name	UniProtKB	Expression
TEKT5	Q96M29	>90%
CMTM2	Q8TAZ6	>90%
ACR	P10323	>90%
PRSS37	A4D1T9	>90%
RGS22	Q8NE09	50% - 75%
HIST1H1T	P22492	>90%
PRKACG	P22612	>90%
CABYR	O75952	75% - 90%
TSKS	Q9UJT2	>90%

s testis enriched, expression must be > 50% in testis in at least 2 databases. Interactors were

Testis YTH identified interactors
Sperm Mass Spectometry identified interactors
Databases retrieved interactors
ssion in testis in at least 2 databases. Interactors were classified in three categories: 50-75%; 7

e classified in three categories: 50-75%; 75%-90 and >90%.

'5%-90 and >90%.

Supplementary Table XI. Te

Gene Name	UniProtKB
BCCIP	Q9P287
HSP90AB1	P08238
RUNX1	Q01196
HSP90AA1	P07900
DCP1B	Q8IZD4
MAEA	Q7L5Y9
SBNO1	A3KN83
NBR1	Q14596
SUGP2	Q8IX01
PSMD8	P48556
MYL12A	P19105
ALKBH3	Q96Q83
HMGN1	P05114
DNAJB1	P25685
DEAF1	O75398
H2AFV	Q71UI9
CCDC174	Q6PII3
TTC16	Q8NEE8
AURKAIP1	Q9NWT8
DDI1	Q8WTU0
SMG7	Q92540
RPL19	P84098
LRRC37A2	A6NM11
C11orf98	E9PRG8
AP3D1	O14617
GOLGA6C	A6NDK9
CNTROB	Q8N137
PTMA	P06454
RPS15	P62841
VCPIP1	Q96JH7
LDHA	P00338
SMARCA5	O60264
LRP6	O75581
DCAF8	Q5TAQ9
FBXO42	Q6P3S6
AXIN2	Q9Y2T1
MTCH1	Q9NZJ7
AKAP11	Q9UKA4

RPL29	P47914
UBTF	P17480
CHTOP	Q9Y3Y2
RPS19	P39019
RPL15	P61313
HNRNPM	P52272
DRC1	Q96MC2
HMBS	P08397
RefSeqGene on chromosome	
Human Dna sequence from cl	
Homo Sapiens Chromosome 2	
ARG1	P05089
GGCT	O75223
HIST1H2AD	P20671
TLR9	Q9NR96
SBSN	Q6UWP8
HIST1H4A	P62805
HIST1H2BK	A0A024RCL8
HSPA5	P11021
RPS18	P62269
ACR	P10323
RPL13	P26373
LTF	P02788
PRSS37	A4D1T9
RPL6	Q02878
CPZ	Q66K79
RPS8	P62241
EEF1G	P26641
AXIN1	O15169-2
CTNNB1	B4DGU4
PKM	P14618-1
AXIN1	O15169
YWHAG	P61981
FRAT1	Q92837
GSKIP	Q9P0R6
MAPT	P10636
PRKACA	P17612

GSK3A	P49840
AIM1	Q9Y4K1
AKAP9	Q99996
AR	P10275
CTNNA1	P35221
PPP1R2	P41236
MDN1	Q9NU22
PSMD1	Q99460
POLR3B	Q9NW08
ZDHHC17	Q8IUH5
AKT1	P31749
PRKCA	P17252
PRKCB	P05771
PRKCD	Q05655
PRKCG	P05129
APP	P05067
ARHGEF11	O15085
PKM	P14618
KRBA1	A5PL33

MAP3K11	Q16584
MYC	P01106
SPICE1	Q8N0Z3
VTA1	Q9NP79
EIF2B5	Q13144
PRKD3	O94806
SGK3	Q96BR1
CTNNB1	P35222
FCGR2B	P31994
HDAC6	Q9UBN7
PPP3CC	P48454
RCAN2	Q14206
SPG21	Q9NZD8
TRAK2	O60296
BICD1	Q96G01
CREM	Q03060
GSK3B	P49841
HSF1	Q00613
PRKCZ	Q05513
MCL1	Q07820
SGK1	O00141
TUBG1	P23258
BCL3	P20749
CREB1	P16220
EBNA1BP2	Q99848
GLI3	P10071
PRKCH	P24723
LRSAM1	Q6UWE0
PXN	P49023

PRKDC	P78527
RAE1	P78406
RICTOR	Q6R327
ARSG	Q96EG1
PPP1CA	P62136
PPP1CB	P62140
PPP1CC	P36873
PPP3CB	P16298
RCAN1	P53805
SAMHD1	Q9Y3Z3
SRBD1	Q8N5C6
FOXM1	Q08050

estis and sperm related phenotypes/diseases/annotations of GSK3α interac

Phenotyope category
Germ cell line abnormalitities
Spermatogenesis abnormalities
Oligozoospermia
Morphological male reproductive system defects
Male infertility
Male infertility
Male infertility

Morphological male reproductive system defects
Morphological male reproductive system defects

Asthenozoospermia and flagellum, cillium and mitochondrial abnormalities

5 Chromosome 5: 150,401,911-150,402,122
one RP11-543N17
21 clone CTD-250 3J9 map p11-q21.1

Male infertility

Male infertility

Spermatogenesis abnormalities
Male infertility

Male infertility
Morphological male reproductive system defects

Asthenozoospermia and flagellum, cillium and mitochondrial abnormalities
Male infertility
Morphological male reproductive system defects

Male infertility
Morphological male reproductive system defects
Other testicular cells abnormalities
Germ cell line abnormalitities
Spermatogenesis abnormalities
Morphological male reproductive system defects
Oligozoospermia
Teratozoospermia
Male infertility

Other testicular cells abnormalities
Spermatogenesis abnormalities
Morphological male reproductive system defects
Germ cell line abnormalitities
Asthenozoospermia and flagellum, cillium and mitochondrial abnormalities
Oligozoospermia
Male infertility
Inflamation of male reproductive system components

Morphological male reproductive system defects

Spermatogenesis abnormalities
Morphological male reproductive system defects
Oligozoospermia
Male infertility

Male infertility

Morphological male reproductive system defects

Male infertility
Asthenozoospermia and flagellum, cillium and mitochondrial abnormalities
Male infertility

Spermatogenesis abnormalities
Morphological male reproductive system defects
Male infertility
Oligozoospermia
Teratozoospermia

Spermatogenesis abnormalities

Morphological male reproductive system defects
Oligozoospermia

Morphological male reproductive system defects

Morphological male reproductive system defects

Spermatogenesis abnormalities
Morphological male reproductive system defects
Asthenozoospermia and flagellum, cillium and mitochondrial abnormalities
Teratozoospermia
Male infertility
Germ cell line abnormalitities
Oligozoospermia
Germ cell line abnormalitities

Male infertility

ctome. Testis and sperm related phenotypes/diseases/a

GeneOntology Annotations
Microtuble-based movement
ATP metabolic process

Locomotion
Cell motility

Locomotion
Cell motility

Locomotion
Cell motility

Locomotion
Cell motility

Cilium

Microtuble-based movement
Sperm capacitation
Motile cilium
Cilium
Sperm flagellum
Spermatogenesis

Locomotion
Cell motility

Spermatogenesis
Cilium movement
Locomotion
Cell motility

Cilium
Locomotion
Cell motility
Locomotion
Cell motility

Locomotion
Cell motility

Microtuble-based movement
Cilium
Locomotion

ATP metabolic process

Locomotion
Cell motility

Microtuble-based movement
Locomotion
Cell motility

Microtuble-based movement
Microtuble-based movement

Spermatogenesis

Spermatogenesis
Microtuble-based movement
Locomotion
Cell motility

Locomotion
Cell motility
Cilium

Locomotion

Axoneme
Locomotion
Cilium
Cell motility

ATP metabolic process

Locomotion

annotations of all GSK3α interactors were retrieved and categorized. Yellow: GSK3α t

Testis YTH identified interactors
Sperm Mass Spectometry identified interactors
Databases retrieved interactors

estis interactors; Green: GSK3α sperm interactors; Orange: GSK3α database

Supplementary Table XII. Te

Gene Name	UniProtKB
MYL6	P60660
DCP1B	Q8IZD4
BCCIP	Q9P287
HSP90AA1	P07900
RPS15	P62841
PSMD8	P48556
C10orf90	Q96M02
TEKT5	Q96M29
YBX1	P67809
CASC4	Q6P4E1
CMTM2	Q8TAZ6
LYAR	Q9NX58
AXIN2	Q9Y2T1
PRKRIP1	Q9H875
HNRNPM	P52272
C11orf98	E9PRG8
SMG7	Q92540
HSP90AB1	P08238
Human DNA sequence from	
ANXA1	P04083
ARG1	P05089
BPIFB1	Q8TDL5
CASP14	P31944
CAT	P04040
CTSG	P08311
LYZ	B2R4C5
DMBT1	Q9UGM3
GGCT	O75223

GSN	P06396
GAPDH	P04406
HP	P00738
HSP90AB1	P08238
HSPA2	P54652
HIST1H2AD	P20671
HIST1H2BK	A0A024RCL8
H3F3B	P84243
HIST1H3A	P68431
HIST1H4A	P62805
MUC5AC	A7Y9J9
MPO	P05164
PFN1	P07737
S100A8	P05109
DKFZp686J11:	Q6MZW0
SERPINB4	P48594
TLR9	Q9NR96
n/a	Q6GMV8
ZG16B	Q96DA0
ACR	P10323
PRSS37	A4D1T9
RPL6	Q02878
RPS18	P62269
LTF	P02788
RPL13	P26373
AXIN1	O15169
MAPT isoform	P10636-8
EGLN3	Q9H6Z9
CABYR isoforn	O75952-5
CABYR isoforn	O75952-3
MAPT isoform	P10636-7
DAB2IP isofor	Q5VWQ8-2
CTNNB1	P35222
APC	P25054
GSK3B	P49841
AKAP11	Q9UKA4

	P31749
TP53	P04637
GSKIP	Q9P0R6
PRKACA	P17612
LRP6	O75581
MYC	P01106
MAPT	P10636
AR	P10275
FRAT1	Q92837
PPP1R2	P41236
MUC1	P15941
NOTCH1	P46531
SGK3	Q96BR1
SMAD3	P84022
SNAI1	O95863
DNM1L	O00429
NIN	Q8N4C6
ACLY	P53396
PPP1CA	P62136
PTPN1	P18031
STRAP	Q9Y3F4
TSC2	P49815

ATXN3	P54252
PSEN1	P49768
PTK2	Q05397
FRAT2	O75474
APP	P05067
GYS1	P13807
PRKAR1A	P10644
PPP1CC	P36873
VIM	P08670
CCNE1	P24864
SMAD1	Q15797
BTRC	Q9Y297
BICD1	Q96G01
EPM2A	B3EWF7
NOTCH2	Q04721
AKT2	P31751
HSPA1A	P0DMV8
HSPA1B	P0DMV9
LRRK2	Q5S007
RELB	Q01201
UBR5	O95071

CABYR	O75952
DEAF1	O75398
DDX20	Q9UHI6
DHX36	Q9H2U1
EWSR1	Q01844
ZFPM1	Q8IX07
GEMIN4	P57678
IGF2BP1	Q9NZI8
SNRNP70	P08621
SF3B1	O75533
SMN1	Q16637
SMYD2	Q9NRG4
XPO6	Q96QU8
KLF5	Q13887
MAP3K1	Q13233
SNAI2	O43623
CDH1	P12830
FZR1	Q9UM11
AURKA	O14965
SP7	Q8TDD2
ANKRD6	Q9Y2G4
CLASP2	O75122
DAB2IP	Q5VWQ8
DYNLL1	P63167
E2F1	Q01094

EPB41L3	Q9Y2J2
PRKAR2A	P13861
PRUNE1	Q86TP1
RPF2	Q9H7B2
RELA	Q04206
TRAF2	Q12933
TANK	Q92844
TSC1	Q92574
MAPK1	P28482
NBR1	Q14596
BCL3	P20749
CCND1	P24385
HSPA4	P34932
NFKB1	P19838
SNCAIP	Q9Y6H5
ARHGEF11	O15085
KRBA1	A5PL33
SFPQ	P23246
SPICE1	Q8N0Z3
VTA1	Q9NP79
EIF2B5	Q13144
JUN	P05412
PRKCB	P05771
CREB1	P16220
DACT1	Q9NYF0
DDIT4	Q9NX09
EYA1	Q99502
FOXO1	Q12778

PRKCA	P17252
PRKCZ	Q05513
MDM2	Q00987
IKBKG	Q9Y6K9
NFE2L1	Q14494
NFE2L3	Q9Y4A8
PHLPP1	O60346
PPARGC1A	Q9UBK2
TAZ	Q16635
WWTR1	Q9GZV5
YWHAZ	P63104
PPP2R5D	Q14738
EIF4EBP1	Q13541
ACACA	Q13085
ACSBG1	Q96GR2
DBI	P07108
ACTL6B	O94805
ACTBL2	Q562R1
ADAP1	O75689
ADIRF	Q15847
PMAIP1	Q13794
ASRGL1	Q7L266
ATF3	P18847
ATPIF1	Q9UII2
BAG6	P46379
BEX1	Q9HBH7
BHLHE41	Q9C0J9
BIRC2	Q13490
BIRC3	Q13489
BRIX1	Q8TDN6
BZW2	Q9Y6E2
CAMSAP3	Q9P1Y5
CCDC6	Q16204

CDC37	Q16543
CEBPB	P17676
CEBPZ	Q03701
CENPB	P07199
CHD3	Q12873
CRELD2	Q6UXH1
CSAD	Q9Y600
CSF3R	Q99062
CSNK2B	P67870
COPS5	Q92905
GJB5	O95377
CSTB	P04080
CST6	Q15828
DCD	P81605
DCTN3	O75935
DDX5	P17844
BHLHE40	O14503
DEC1	Q9P2X7
DEFA1	P59665
HSD17B4	P51659
DHX34	Q14147
DNAJC13	O75165
DNMT3L	Q9UJW3
DNMT1	P26358
DUSP9	Q99956
EEF1A1	P68104
EEF1G	P26641
ELAVL1	Q15717
IKBKAP	O95163
MPP1	Q00013

ENTPD6	O75354
C14orf1	Q9UKR5
PFKFB4	Q16877
FAM83D	Q9H4H8
FBN3	Q75N90
FBXW11	Q9UKB1
FBXW7	Q969H0
FEN1	P39748
IFT46	Q9NQC8
VPS51	Q9UID3
FIBP	O43427
FIP1L1	Q6UN15
FKBP14	Q9NWM8
KHSRP	Q92945
FUS	P35637
FZD5	Q13467
GAPDH	P04406
GNB2	P62879
GBP2	P32456
GIPC1	O14908
GPR39	O43194
HSPA9	P38646
HSPA5	P11021
HIST1H1C	P16403
HIST1H1E	P10412
HIST1H1T	P22492
H1FX	Q92522
HAX1	O00165
HBA1	P69905
HDAC6	Q9UBN7
HECW2	Q9P2P5
HRNR	Q86YZ3
HP	P00738
HSPA8	P11142
CLNS1A	P54105

IGHM	P01871
IGSF21	Q96ID5
ILK	Q13418
IQCG	Q9H095
ITLN1	Q8WWA0
KANK1	Q14678
KIF5B	P33176
LUC7L2	Q9Y383
LMO4	P61968
MID1IP1	Q9NPA3
MAP3K11	Q16584
MAP1A	P78559
MAP4	P27816
MASP1	P48740
MCCC2	Q9HCC0
MED24	O75448
MICAL1	Q8TDZ2
MKL1	Q969V6
MAP2K5	Q13163
MTF2	Q9Y483
MTOR	P42345
MYCN	P04198
MYH9	P35579
NAT9	Q9BTE0
MGEA5	O60502
NOTCH3	Q9UM47
NRBP1	Q9UHY1
IVNS1ABP	Q9Y6Y0

NSFL1C	Q9UNZ2
NUB1	Q9Y5A7
NUFIP1	Q9UHK0
KIAA1191	Q96A73
PIM2	Q9P1W9
PPP3CC	P48454
PRDX1	Q06830
PTBP3	O95758
PTN	P21246
QPCTL	Q9NXS2
RAI1	Q7Z5J4
RASSF1	Q9NS23
RCAN2	Q14206
UPF3A	Q9H1J1
RGS22	Q8NE09
RPL13	P26373
RPL19	P84098
RPL23	P62829
RPL23A	P62750
RPL27A	P46776
RPL29	P47914
RPL31	P62899
RPL35	P42766
RPL36A	P83881
RPL36AL	Q969Q0
RPL37	P61927
RPL37A	P61513
RPL8	P62917
RPLP1	P05386
RNF220	Q5VTB9
POLR2B	P30876
RPS11	P62280
RPS14	P62263
RPS16	P62249
RPS17	P08708
RPS18	P62269
RPS19	P39019
RPS23	P62266
RPS24	P62847
RPS25	P62851
RPS27A	P62979
RPS29	P62273

RPS2	P15880
FAU	P35544
RPS4X	P62701
RPS6	P62753
RSU1	Q15404
RXRA	P19793
SAP30BP	Q9UHR5
SF3A1	Q15459
SHROOM3	Q8TF72
SLA	Q13239
SMARCA2	P51531
SMARCA5	O60264
SMURF2	Q9HAU4
SPTBN4	Q9H254
STK11	Q15831
RBPJ	Q06330
SYNE4	Q8N205
EPRS	P07814
QARS	P47897
TUBA1A	Q71U36
TUBB1	Q9H4B7
TUBB	P07437
TBC1D4	O60343
CLEC3B	P05452
TLE1	Q04724
TMEM44	Q2T9K0
TONSL	Q96HA7
TOP2A	P11388
PBK	Q96KB5
TRAK2	O60296
TRAP1	Q12931
HSP90B2P	Q58FF3
TRIM29	Q14134
PRSS3	P35030
EFTUD2	Q15029
UBE2D1	P51668
UBR1	Q8IWV7
UBXN6	Q9BZV1

UFM1	P61960
WSB1	Q9Y6I7
XIAP	P98170
ERCC4	Q92889
XPO1	O14980
XPNPEP1	Q9NQW7
YAP1	P46937
ZHX1	Q9UKY1
ZKSCAN2	Q63HK3
ZNF135	P52742
ZNF227	Q86WZ6
ZNF746	Q6NUN9
HNRNPD	Q14103
YBX3	P16989
SNCA	P37840
CREM	Q03060
DPYSL2	Q16555
GSK3A	P49840
MCL1	Q07820
MYOCD	Q8IZQ8
OGT	O15294
PCM1	Q15154
MBD1	Q9UIS9
SGK1	O00141
TUBG1	P23258
TPPP	O94811
AKT3	Q9Y243
ARRB1	P49407
BICD2	Q8TD16
CIITA	P33076
CDK5	Q00535
CDX2	Q99626

CEBPA	P49715
CREB3L3	Q68CJ9
CTNND1	O60716
DYNC1I1	O14576
DCTN1	Q14203
DCTN2	Q13561
HDAC4	P56524
KLF2	Q9Y5W3
RPS6KA1	Q15418
MAP3K4	Q9Y6R4
MAP1B	P46821
MARK2	Q7KZI7
MITF	O75030
NCOA3	Q9Y6Q9
NFE2L2	Q16236
PIK3R1	P27986
PXN	P49023
PDE4D	Q08499
PRKDC	P78527
RCAN1	P53805
RICTOR	Q6R327
SREBF1	P36956
TMEM132A	Q24JP5
FZD1	Q9UP38
GRB14	Q14449
ILKAP	Q9H0C8
MAP2K7	O14733
PPP2CA	P67775

PTPN11	Q06124
AMMECR1	Q9Y4X0
STYK1	Q6J9G0
YWHAQ	P27348
APC2	O95996
APOC2	P02655
SLC25A23	Q9BV35
ANAPC2	Q9UJX6
CDKN1B	P46527
CREB3	O43889
DVL2	O14641
DVL3	Q92997
GLI2	P10070
GYS2	P54840
PRKACG	P22612
PIN1	Q13526
PRKX	P51817
TSKS	Q9UJT2
CD274	Q9NZQ7
PIAS1	O75925
DEFA5	Q01523
DKK3	Q9UBP4
KIAA0317	O15033
MAP3K2	Q9Y2U5
NFATC1	O95644
NFATC2	Q13469
PPP1CB	P62140
SAMHD1	Q9Y3Z3
TBK1	Q9UHD2
U2AF1	Q01081
UBE3A	Q05086

UBXN2B	Q14CS0
SOX10	P56693
LPCAT1	Q8NF37
SOX9	P48436
FOXM1	Q08050

estis and sperm related phenotypes/diseases/annotations of GSK3β inte

Phenotyope category

Germ cell line abnormalitities
Spermatogenesis abnormalities
Oligozoospermia
Morphological male reproductive system defects
Male infertility

clone RP11-543N17 on chromosome 10, complete sequence

Oligozoospermia
Asthenozoospermia and flagellum, cillium and mitochondrial abnormalities
Male Infertility

Spermatogenesis abnormalities
Morphological male reproductive system defects
Male infertility

Spermatogenesis abnormalities
Male infertility
Spermatogenesis abnormalities
Male infertility

Male infertility
Spermatogenesis abnormalities
Male infertility

Male infertility
Morphological male reproductive system defects

Male infertility

Spermatogenesis abnormalities
Morphological male reproductive system defects
Oligozoospermia
Oligozoospermia
Male Infertility

Asthenozoospermia and flagellum, cillium and mitochondrial abnormalities
Male infertility
Morphological male reproductive system defects

Male infertility
Other testicular cells abnormalities

Other testicular cells abnormalities
Spermatogenesis abnormalities
Morphological male reproductive system defects
Germ cell line abnormalitities
Asthenozoospermia and flagellum, cillium and mitochondrial abnormalities
Oligozoospermia
Male infertility
Inflamation of male reproductive system components

Male infertility

Morphological male reproductive system defects
Other testicular cells abnormalities
Spermatogenesis abnormalities
Germ cell line abnormalitities

Male infertility

Male infertility

Male infertility
Morphological male reproductive system defects
Spermatogenesis abnormalities
Morphological male reproductive system defects
Asthenozoospermia and flagellum, cillium and mitochondrial abnormalities
Teratozoospermia
Male infertility
Germ cell line abnormalitities
Oligozoospermia
Germ cell line abnormalitities
Male infertility
Male infertility
Morphological male reproductive system defects
Male infertility

Male infertility
Spermatogenesis abnormalities
Oligozoospermia

Morphological male reproductive system defects

Inflamation of male reproductive system components
Male infertility

Morphological male reproductive system defects
Oligozoospermia
Male hormonal abnormalities
Male infertility

Male infertility
Morphological male reproductive system defects

Asthenozoospermia and flagellum, cillium and mitochondrial abnormalities
Oligozoospermia
Male Infertility

Other testicular cells abnormalities
Morphological male reproductive system defects
Oligozoospermia
Male Infertility

Male infertility

Male infertility

Morphological male reproductive system defects
Other testicular cells abnormalities
Spermatogenesis abnormalities
Germ cell line abnormalitities

Male infertility
Germ cell line abnormalitities
Morphological male reproductive system defects
Spermatogenesis abnormalities
Asthenozoospermia and flagellum, cillium and mitochondrial abnormalities
Male infertility
Oligozoospermia

Morphological male reproductive system defects
Oligozoospermia

Male infertility

Male Infertlity

Male infertility
Male infertility
Oligozoospermia

Male infertility
Spermatogenesis abnormalities
Morphological male reproductive system defects
Germ cell line abnormalitities
Oligozoospermia
Male infertility
Male infertility

Other testicular cells abnormalities
Male infertility
Male hormonal abnormalities
Male infertility

Male infertility

Male infertility

Oligozoospermia
Morphological male reproductive system defects
Male infertility

Male infertility

Morphological male reproductive system defects

Morphological male reproductive system defects
Spermatogenesis abnormalities
Germ cell line abnormalitities
Male infertility

Morphological male reproductive system defects
Spermatogenesis abnormalities
Oligozoospermia
Germ cell line abnormalitities
Male infertility
Oligozoospermia
Male Infertility

Male infertility

Spermatogenesis abnormalities
Male infertility
Morphological male reproductive system defects
Oligozoospermia

Male infertility

Male infertility
Oligozoospermia

Male infertility
Morphological male reproductive system defects

Male infertility

Spermatogenesis abnormalities
Asthenozoospermia and flagellum, cillium and mitochondrial abnormalities
Oligozoospermia
Male infertility
Teratozoospermia

Morphological male reproductive system defects

Male infertility

Male infertility

Male infertility
Morphological male reproductive system defects

Asthenozoospermia and flagellum, cillium and mitochondrial abnormalities
Male infertility

Male infertility

Male infertility

Morphological male reproductive system defects

Morphological male reproductive system defects

Morphological male reproductive system defects

Morphological male reproductive system defects

Morphological male reproductive system defects

Male infertility

Male infertility
Morphological male reproductive system defects

Male infertility
Morphological male reproductive system defects
Other testicular cells abnormalities
Spermatogenesis abnormalities
Germ cell line abnormalitities
Male infertility

Morphological male reproductive system defects

Male infertility
Morphological male reproductive system defects
Male infertility

Male infertility

Spermatogenesis abnormalities
Morphological male reproductive system defects
Male infertility
Oligozoospermia
Teratozoospermia

Male infertility

Male infertility

Morphological male reproductive system defects
Asthenozoospermia and flagellum, cillium and mitochondrial abnormalities
Male infertility
Oligozoospermia

Male infertility
Morphological male reproductive system defects
Male infertility
Male infertility
Morphological male reproductive system defects
Male infertility
Asthenozoospermia and flagellum, cillium and mitochondrial abnormalities
Male Infertility

Male infertility
Morphological male reproductive system defects

Male infertility

Male infertility

Male infertility
Morphological male reproductive system defects
Spermatogenesis abnormalities
Male infertility

Morphological male reproductive system defects
Male infertility

Male infertility

Morphological male reproductive system defects
Morphological male reproductive system defects
Germ cell line abnormalitities
Oligozoospermia

Morphological male reproductive system defects
Male Infertility

Oligozoospermia
Morphological male reproductive system defects
Male infertility

Morphological male reproductive system defects
Oligozoospermia
Male infertility

Morphological male reproductive system defects
Male infertility

Morphological male reproductive system defects
Oligozoospermia
Male infertility
Male hormonal abnormalities
Other testicular cells abnormalities

eractome. Testis and sperm related phenotypes/diseases/annotations of all GSK3β inte

GeneOntology Annotations

Motile cilium
Microtuble-based movement
Sperm motility
Cilium movement
Cilium
Sperm flagellum
Locomotion
Cell motility

Locomotion

Locomotion
Cell motility
ATP metabolic process

Spermatogenesis

Locomotion
Cell motility
Locomotion
Cell motility

Locomotion
Cell motility

Locomotion
Cell motility
Locomotion
Cell motility

Cilium
Locomotion
Cell motility

Motile cilium
Cilium
Sperm flagellum
Spermatogenesis

Microtuble-based movement

Spermatogenesis

Spermatogenesis
Locomotion
Cell motility
Locomotion
Cell motility
Locomotion
Cell motility
Locomotion
Cell motility
ATP metabolic process
Cilium

Locomotion
Cell motility

Locomotion

Cilium
Locomotion
Cell motility
Locomotion
Cell motility

Microtuble-based movement
Cilium
Locomotion

Cilium

Microtuble-based movement

Locomotion
Cell motility
ATP metabolic process
ATP metabolic process
Locomotion
Cell motility

Sperm capacitation
Motile cilium
Microtuble-based movement
Cilium movement
Cilium
Sperm flagellum
Spermatogenesis

Locomotion
Cell motility

Cilium

Locomotion
Cell motility
Locomotion
Cell motility

Microtuble-based movement
Cilium

Spermatogenesis

Cilium

Locomotion
Cell motility

Locomotion
Cell motility

Locomotion

ATP metabolic process
Locomotion
Cell motility

Locomotion
Cell motility
Microtuble-based movement
Locomotion
Cell motility
Locomotion
Cell motility

ATP metabolic process
Locomotion
Cell motility

ATP metabolic process

ATP metabolic process
Spermatogenesis

Spermatogenesis

Locomotion
Cell motility
Cilium
Locomotion
Cell motility

Locomotion
Cell motility

Spermatogenesis

Locomotion
Cell motility
Locomotion
Cell motility

ATP metabolic process
Locomotion
Cell motility

Motile cilium
Cilium

Locomotion
Cell motility

Locomotion
Cell motility

Spermatogenesis

Microtuble-based movement
Locomotion
Cell motility

ATP metabolic process

Locomotion
Cell motility

Locomotion
Cell motility
Motile cilium
Sperm motility
Cilium
Sperm flagellum
Spermatogenesis
Locomotion
Cell motility

Locomotion
Cell motility
Microtuble-based movement
Cilium
Locomotion

Locomotion
Cell motility

Axoneme
Microtuble-based movement
Cilium

Microtuble-based movement

Locomotion
Cell motility

Locomotion
Cell motility

Locomotion
Cell motility

Spermatogenesis

Locomotion
Cell motility

Locomotion
Cell motility

Locomotion
Cell motility

Spermatogenesis

Locomotion
Cell motility
Locomotion

Spermatogenesis

Microtuble-based movement

Locomotion
Cell motility

ATP metabolic process
Spermatogenesis
Locomotion

Spermatogenesis
Locomotion
Locomotion
Cell motility

Locomotion
Cell motility
ATP metabolic process
Microtuble-based movement
Cilium
Locomotion
Cell motility

Locomotion
Cell motility
Cilium

Microtublle-based movement

Locomotion
Cell motility

Microtuble-based movement
Microtuble-based movement

ATP metabolic process
Locomotion
Cell motility

Microtuble-based movement
Cilium
Locomotion
Cell motility

Locomotion
Cell motility
Locomotion
Cell motility

Locomotion
Cell motility

Locomotion
Cell motility

Locomotion
Cell motility

Locomotion
Cell motility

ATP metabolic process

Locomotion
Cell motility

Axoneme
Motile cilium
Cilium
Locomotion

Cilium
Spermatogenesis

Locomotion
Cell motility
Locomotion
Cell motility
Cilium movement
Locomotion
Cell motility
Spermatogenesis

Locomotion
Cell motility

Locomotion
Cell motility

Spermatogenesis
Locomotion
Cell motility

eractors were retrieved and categorized. Yellow: GSK3β testis interactors; Green: GSK3β sperm in

	Testis YTH identified interactors
	Sperm Mass Spectometry identified interactors
	Databases retrieved interactors

ıteractors; Orange: GSK3β database interactors.